

UTILIZATION OF RECYCLED CARBIDE AS ADSORBENT FOR ADSORPTION OF DYES AND COD FROM TEXTILE WASTE

Muhammad Arief KARIM[✉], Henny YUNIAR, Kharien Hemalia Putri RABIA

Faculty of Engineering, Muhammadiyah University of Palembang, Jl. Ahmad Yani 13 Ulu, 30263 Palembang, Indonesia

Highlights:

- **Optimal Absorption Conditions:** At 90 minutes, with a mass of 7.5 g, the absorption of Jumputan fabric liquid waste peaked at 95.95%, while color intensity absorption reached 97.99%. This demonstrates the effectiveness of absorption, with subsequent increases attributed to increased liquid waste content;
- **Saturation Point:** Absorption decreased from 120 to 210 minutes, indicating adsorbent saturation, wherein no significant changes in absorption occurred. This highlights the limitation of the adsorption process over prolonged contact times;
- **Influence of Adsorbent and Contact Time:** The significant increase in COD and color reduction percentages underscores the impact of adsorbent mass and contact time. Initial rapid absorption suggests effective surface adsorption, while saturation implies the necessity for diffusion through adsorbent pores for further reduction;
- **Kinetic Model Suitability:** The pseudo-second-order kinetic model is appropriate for both decolorization and COD reduction, with high R^2 values of 0.994 and 0.993, respectively. This indicates a strong correlation between experimental and theoretical values, validating the model's applicability;
- **Isotherm Model Fit:** The Langmuir Isotherm Model is well-suited for COD reduction, exhibiting an R^2 value of 0.9918, while color removal aligns better with the Freundlich isotherm model, reflecting an R^2 value of 0.9633. This suggests varying adsorption mechanisms for different pollutants and emphasizes the importance of selecting appropriate models for accurate prediction and understanding of the adsorption process.

Article History:

- received 04 April 2024
- accepted 13 January 2025

Abstract. This study assessed the potential of carbide waste (CW), a by-product of the welding industry, as a cost-effective adsorbent for removing dyes and COD from textile wastewater. CW was prepared through drying, filtering, and shaping into 2 mm-thick tablets (3 mm diameter), followed by heating at 150 °C for 120 minutes. Characterization using FTIR and SEM-EDX confirmed functional groups like hydroxyl and carbonyl and significant surface morphological changes. Batch experiments achieved maximum color and COD removal efficiencies of 94.48% and 96.73%, respectively, at 75 g adsorbent dosage and 150 min contact time. Freundlich isotherm ($R^2 = 0.9918$ for color) indicated heterogeneous adsorption, and kinetic studies fit a pseudo-second-order model. The process was exothermic, spontaneous, and governed by physical adsorption. Regeneration trials showed COD removal efficiency remained 90% after four cycles. These findings establish CW as an efficient, sustainable adsorbent with promising environmental and industrial applications for textile wastewater treatment.

Keywords: textile wastewater, CW adsorbent, adsorption, color removal, COD reduction.

✉ Corresponding author. E-mail: ariefkarim8@gmail.com

1. Introduction

The rapid industrial development in the modern era has significantly impacted the environment, particularly in urban, rural, and aquatic areas. Water, as a vital element for life and ecosystems, is increasingly threatened by various pollutants, including heavy metals, organic substances, pesticides, drugs, and dyes (Mostafapour et al., 2022; Kalavathy et al., 2009; Maldonado et al., 2006). Palembang, South Sumatra, is known as a producer of Jumputan fabric, which in its production process requires the use of various types of dyes.

Textile industry waste containing dyes can reduce sunlight penetration into water bodies, which is essential for the photosynthesis process of aquatic biota. This harms

the balance of aquatic ecosystems (Lambert & Davy, 2011; Aichour et al., 2021). The waste from Jumputan fabric production also contains various hazardous pollutants, such as toxic substances, oils, fats, COD, BOD, sulfides, suspended solids (SS), and dark, concentrated colors (Gao et al., 2007; Chen et al., 2003; Georgiou et al., 2005).

Synthetic dyes, commonly found in textile, leather, and paper industry wastewater, come in a variety of types, each with different effects on ecological systems and human well-being. Frequently used colorants include azo dyes, acidic colorants, dispersed pigments, reactive dyes, and basic colorants. Azo dyes are the largest group used in the textile and leather industries, known for their high color fastness (Balarak et al., 2020a).

However, some azo dyes can degrade into carcinogenic aromatic amines that can contaminate water sources and pose health risks (Lambert & Davy, 2011; Aichour et al., 2021). Acid dyes are used for dyeing wool, silk, and nylon; although generally non-toxic, these dyes can affect water quality by altering pH and reducing dissolved oxygen levels, ultimately harming aquatic life.

Disperse dyes, used to dye synthetic fibers such as polyester, have very small particle sizes that can disperse in water without dissolving. These dyes often cause skin allergies and respiratory issues in textile industry workers. In the environment, these dyes can settle at the bottom of rivers and lakes, poisoning aquatic organisms (Lambert & Davy, 2011; Aichour et al., 2021). Reactive dyes, used to dye cotton and other cellulose fibers, form covalent bonds with the fibers, producing very durable colors. However, these dyes can cause skin irritation and respiratory problems if inhaled as dust, and the waste containing these dyes is difficult to treat due to their high stability (Lambert & Davy, 2011; Aichour et al., 2021).

When synthetic dyes are released into the environment without adequate treatment, they can cause various environmental and health problems. In water bodies, dyes can block sunlight penetration, inhibit photosynthesis, and disrupt the balance of aquatic ecosystems. Some dyes can also interfere with biochemical processes in water, leading to reduced oxygen levels that endanger aquatic life (Forgacs et al., 2004). From a human health perspective, long-term exposure to these dyes, whether through contaminated drinking water or direct contact during production processes, can cause various health issues, including cancer, skin irritation, allergies, and dysfunctions of vital organs such as the kidneys reproductive system, liver function, neurological system, and central nervous system (Zhou et al., 2019; Rauf & Ashraf, 2012; Kadirvelu et al., 2003).

The control and treatment of dye-containing waste are crucial to minimize these negative impacts. Research is ongoing to develop more effective wastewater treatment methods, such as adsorption using natural biosorbents, advanced oxidation, and electrocoagulation, to ensure that the release of industrial waste into the environment can be carried out safely and sustainably (Balarak et al., 2019, 2020b).

Various methods have been developed to remove dye contaminants from aqueous solutions, as reported in several studies. One widely used method is adsorption, where single-walled carbon nanotubes (SWCNTs) have been proven effective in adsorbing Acid Blue 92 dye from solutions, with isothermal, kinetic, and thermodynamic analyses showing high efficiency of this process (Ajayan et al., 2020). Additionally, biosorption using canola waste as a biosorbent has shown promising results in removing Acid Orange 7, with studies evaluating biosorption equilibrium and operational parameters that affect its effectiveness (Smith et al., 2021). Another innovative method is the use of sonophotocatalytic processes, which combine ultrasonic and photocatalysis with titanium dioxide nanocomposites and graphene oxide for the degradation of Acid Orange 7, demonstrating enhanced degradation through variations

in process parameters (Lee et al., 2019). The application of nano zerovalent iron on carbon-based support has proven effective in treating complex organic wastewater such as melanoidin, showing substantial improvement in color and COD removal efficiency (Raji et al., 2021). Electrochemical and bio-electrochemical methods have been shown to be effective in treating industrial yeast effluents, as demonstrated by Liakos et al. (2017).

Furthermore, adsorption using surfactant-modified bentonite has been used to remove Acid Red 88, where the evaluation of adsorption capacity shows that this modification improves the adsorbent's performance under different operational conditions (Kumar et al., 2010a). Biosorption has also been applied using the aquatic plant *Azolla filiculoides* as an effective and economical biosorption agent for removing Reactive Black 5 from wastewater, showing great potential in textile wastewater treatment (Garcia et al., 2023). Other studies highlight the importance of operational factors such as solution pH, duration of contact, and starting concentration in influencing the efficiency of Acid Blue 25 dye removal from solutions, which is key in optimizing the contaminant removal process (Almeida et al., 2009). The combination of these various methods demonstrates a comprehensive and diverse approach to dealing with dye waste, with results varying depending on the specific conditions applied.

Adsorption methods have gained widespread attention due to their effectiveness and relatively low cost. Utilizing affordable adsorbents derived from industrial by-products and natural sources has proven to be an efficient approach to lowering the concentration of dyes and other hazardous chemicals in wastewater (Adegoke & Bello, 2015; Zhou et al., 2019). Research indicates that a range of materials, including carbon-based adsorbents, modified bentonite, and plant-derived waste, can be effectively employed in the adsorption process to eliminate different types of dyes from textile wastewater (Pirkarami & Olya, 2017; Yagub et al., 2014).

Agricultural waste materials have been widely recognized as cost-effective and efficient adsorbents for the treatment of dye and metal contaminated wastewater (Farhadi et al., 2021). Bamboo-based activated carbon has shown high potential in removing COD and color from textile wastewater, especially from cotton dyeing wastewater (Ahmad & Hamid, 2009). Activated carbon derived from prickly pear seed pulp has been shown to be effective in removing dyes when optimized using experimental design techniques (El Maguana et al., 2019). For example, Devre et al. (2023) developed a sustainable and recyclable biopolymer hydrogel-based adsorbent for the removal of pharmaceutical contaminants, especially tetracycline (TC), from environmental water and industrial wastewater. The utilization of limestone and activated carbon has shown promising results in reducing COD and color levels in textile wastewater (Dhas, 2006). Patil et al. (2020) utilized sugarcane molasses and sea sand to produce carbon composites that were effective in removing methylene blue from textile wastewater. In addition, Babara et al. (2019) successfully converted used toner powder into

Fe₂O₃-g-C₃N₄-based magnetic catalyst, which combines e-waste management with sustainable wastewater treatment at low cost and high efficiency. Another study by Patil et al. (2019) utilized tea residue as a low-cost adsorbent to remove pharmaceutical pollutants such as hydralazine hydrochloride without the need for additional activation. Furthermore, Shinde et al. (2023) used firecracker waste to produce mesoporous carbon and ZnO-MC nanocomposites, which showed high efficiency in the photocatalytic degradation of methyl orange dye. Integration of sonophotocatalysis with nanomaterials such as TiO₂/graphene oxide has shown significant potential in the dye degradation process (Al-Musawi et al., 2021).

In addition to adsorption, other techniques such as electrochemical oxidation and electrocoagulation have also been proposed as solutions to address waste that is difficult to treat with conventional methods. The combination of these methods is often necessary to achieve wastewater treatment levels that meet national discharge standards, given the complexity of the chemical composition in industrial wastewater (Adegoke & Bello, 2015; Zhou et al., 2019).

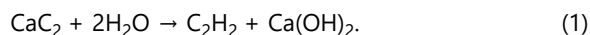
This study utilizes carbide waste (CW) from the welding industry as an innovative and cost-effective adsorbent for textile wastewater treatment. CW, as an industrial byproduct, offers a sustainable solution by utilizing waste that would otherwise become an environmental pollutant.

This study aims to explore the use of CW for the adsorption of dyes and COD from Jumputan fabric wastewater and to investigate the adsorption kinetics and isotherms involved. It is anticipated that the findings of this research will help mitigate the environmental impact of the textile industry and provide a cost-effective alternative to conventional adsorbents.

The unique aspect of this research is the utilization of CW from the welding industry as an innovative and cost-effective adsorbent for textile wastewater treatment. Unlike conventional adsorbents such as activated carbon, CW is an industrial byproduct, providing a sustainable solution by repurposing waste materials that would otherwise contribute to environmental pollution. This study pioneers the use of CW, particularly for the adsorption of dyes and COD from Jumputan fabric wastewater, an area that has been largely unexplored in previous research. Additionally, this study investigates adsorption kinetics and isotherms, providing a comprehensive understanding of the adsorption mechanisms involved. The findings of this research on the effective use of CW in real wastewater treatment applications can significantly reduce the environmental footprint of the textile industry while offering a low-cost alternative to traditional adsorbents.

Calcium carbide waste (CW) is a byproduct derived from the production of acetylene gas (C₂H₂) through the welding process. The primary material consists of lime (Ca(OH)₂), a caustic white solid in its pure form. The reaction between calcium carbide and water, as described in Equation (1), produces acetylene gas used in welding and generates Ca(OH)₂ waste. CW adsorbent is a waste

product from the production of acetylene gas (C₂H₂), as illustrated by the following equation:



Acetylene gas (C₂H₂) is widely used in the ripening of agricultural fruits and industrial welding. However, CW is often discarded in landfills, posing environmental hazards.

According to Jiang (2016), combustion residues from the carbide welding industry have a very high alkalinity (pH 12.84), a specific gravity of 2.32, a specific surface area of 24.664 m²/g, and a clay particle size distribution of 42% for particles smaller than 0.002 mm. Meanwhile, silt particles with sizes ranging from 0.002 to 0.074 mm account for 67.6%, and sand particles larger than 0.074 mm make up 28.2%. CW is carelessly disposed of by welders in the surrounding environment of Palembang. The individual management of carbide welding workshops for metal joining has developed significantly.

A survey conducted in one of the welding industry areas on Jl. Candi Welan, Palembang, revealed around 45 carbide welding workshops. It is estimated that each workshop produces 15 kg of carbide waste per day, so a single carbide welding industrial area could generate 15 tons of carbide waste per year. The solid waste analysis from carbide welding workshops in Surabaya showed that the waste contains 71.58% CaO, 0.76% SiO₂, 2.85% Al₂O₃, and 24.81% other compounds (Karim et al., 2023). Depending on its characteristics, CW can be an effective option as an adsorbent in textile wastewater treatment. To date, research on the use of CW as an adsorbent in the adsorption process for color removal and COD reduction has not been extensively developed. Therefore, it is necessary to conduct studies on the potential of CW as a novel adsorbent for use in treating waste from Jumputan fabric production.

This study aims to utilize CW for the removal of dyes and the reduction of COD in Jumputan fabric wastewater. The influence of environmental conditions, including adsorbent mass, dye concentration, COD, contact time, and solution pH, was also investigated. Additionally, surface characterization, including SEM, EDX, and FTIR, of CW adsorbent is reported. Lastly, we estimated the pseudo-first-order and pseudo-second-order kinetics, as well as commonly used adsorption isotherm studies, to determine the adsorption capacity of CW adsorbent.

2. Methodology

2.1. Materials and equipment

The materials used in this study are CW, Jumputan fabric water waste, and aquaades. The equipment used is a balance, an Erlenmeyer flask, a stirrer, filter paper, and a strainer. Before the adsorption process, the chemical composition and molecular structure of the material were analyzed using Fourier Transform Infrared Spectroscopy (FTIR) and Scanning Electron Microscopy with Energy Dispersive X-ray Spectroscopy (SEM-EDX). After the batch adsorption process is completed, the treated wastewater is filtered

through filter paper with 0.45 μm pores before being analyzed. The color intensity and COD concentration were measured using the DR2800 spectrophotometer (CECIL 1000 series, Cambridge, UK) at a wavelength of 455 nm for color and 600 nm for COD, according to the guidelines set out in the Standard Methods for the Examination of Water and Wastewater (American Public Health Association, 2017).

2.2. Adsorbent preparation

The research process began by drying 12 kg of carbide waste until completely dry, then soaked in distilled water for 24 hours to remove dirt and mineral content. After soaking, the carbide was dried again until completely dry. The dried carbide waste was then ground and sieved with a size of 100 mesh, then molded into tablets with a thickness of 2 mm and a diameter of 3 mm. After being dried in an oven at a temperature of 150 $^{\circ}\text{C}$ for 120 minutes. The weight of one dry tablet is 0.5 grams. Dried in an oven at a temperature of 150 $^{\circ}\text{C}$ for 120 minutes and the adsorbent can be used. The complete visualization of calcium carbide adsorbent preparation is shown in Figure 1.

2.3. Research procedure

The batch process was conducted to comprehensively evaluate and measure the adsorption capacity of carbide waste. The composition of carbide before use in welding consists of 80% CaC_2 , 15% CaO , and 5% other substances, produced by PT. EMDEKI UTAMA Tbk. According to previous research, the primary chemical composition of carbide waste is 71.58% CaO , 0.76% SiO_2 , 2.85% Al_2O_3 , and 24.6% other elements (Arief et al., 2023). With a high CaO content, carbide waste is expected to have a good adsorption capacity for removing color and reducing COD levels from Jumputan textile waste. The Jumputan fabric waste samples used had a COD concentration of 34.589 mg/L and a color index of 45.591 Pt/Co per 100 mL.

For the experiment, three 250 mL Erlenmeyer flasks were prepared. The effect of adsorbent mass on color change and COD reduction was tested by adding 2.5 g, 3.5 g, 4.5 g, 6.0 g, and 7.5 g of carbide waste to each 100 mL sample. Stirring was carried out at a speed of 100 rpm for periods of 30, 60, 90, 120, 150, 180, and 210 minutes.

Additionally, the effect of other operational parameters was studied by varying one parameter while keeping the others constant. The effect of pH was assessed using a consistent initial concentration, an adsorbent dose of 7.5 g, and a contact time of 120 minutes. The pH variation was conducted from pH 2 to pH 12, with adjustments made using dilute NaOH or HCl solutions to regulate the pH. The amount of adsorption at equilibrium, q_e , was calculated using Equation (2):

$$q_e = \frac{(C_o - C_e) \times V}{m}, \quad (2)$$

where q_e (mg/g) represents the amount of dye adsorbed per gram of CW, V (mL) is the initial volume of the dye solution, and m (g) represents the mass of the adsorbent. The percentage removal of color and COD adsorbed by CW was determined using Equation (3):

$$\%R = \frac{C_o - C_t}{C_o} \times 100\%, \quad (3)$$

where C_o and C_t (mg/L) represent the initial and final concentrations of the dye solution.

2.4. Process adsorption

Adsorption is a process in which molecules, ions, or particles from a fluid (either gas or liquid) adhere to the surface of a solid or liquid substance known as an adsorbent. The adsorption mechanism can be categorized into two main types: physical adsorption (physisorption) and chemical adsorption (chemisorption). Physisorption occurs due to Van der Waals forces between the adsorbate molecules

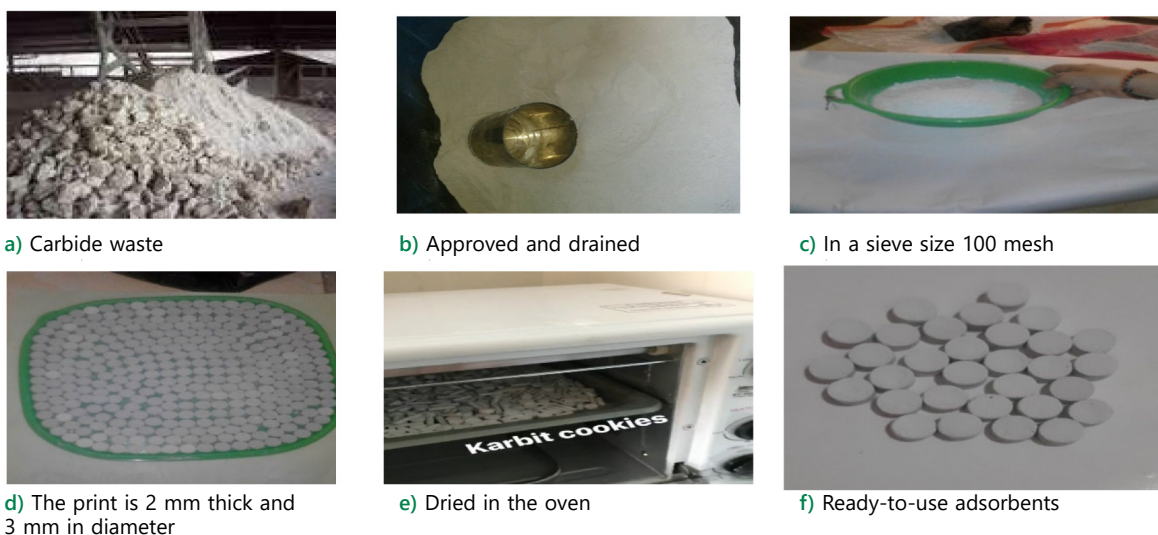


Figure 1. The calcium carbide adsorbent preparation

and the adsorbent surface. This process is reversible, involves relatively low adsorption energy, typically in the range of 20–40 kJ/mol, and is not specific to the type of adsorbate or adsorbent. On the other hand, chemisorption involves the formation of chemical bonds, such as covalent or ionic bonds, between the adsorbate molecules and the adsorbent surface. This process is generally irreversible, with higher adsorption energy, ranging from 80–200 kJ/mol, and is specific to the types of adsorbate and adsorbent interacting (Foo & Hameed, 2010; Toth, 2002).

The stages in the adsorption process include external diffusion, where adsorbate molecules move towards the adsorbent surface, surface adsorption, intraparticle diffusion, and eventually reaching adsorption equilibrium. External diffusion is influenced by concentration gradients, temperature, and pressure, while intraparticle diffusion occurs when adsorbate molecules diffuse into the pores of the adsorbent (Weber & Morris, 1963; McKay et al., 1980). Adsorption equilibrium is reached when the rates of adsorption and desorption balance each other. This adsorption process is often analyzed using various isotherm models, such as the Langmuir model, which assumes adsorption on a homogeneous site with a monolayer of adsorbate, the Freundlich model, which describes adsorption on a heterogeneous surface, and the Dubinin-Radushkevich (D-R) model, which is used to distinguish between physical and chemical adsorption based on adsorption energy (Langmuir, 1918; Freundlich, 1906; Dubinin & Radushkevich, 1947).

Various factors influence the effectiveness of the adsorption process, including the properties of the adsorbent (such as surface area and chemical characteristics), the properties of the adsorbate (such as molecular size and

polarity), the initial concentration of the adsorbate, temperature, and the pH of the solution. For instance, increasing temperature tends to reduce the efficiency of physisorption but may enhance chemisorption (Kumar et al., 2010b). A thorough understanding of the mechanisms and factors affecting adsorption is crucial for optimizing the use of adsorbents in various applications, such as water and wastewater treatment, air purification, the pharmaceutical industry, as well as the food and beverage industry. This understanding also enables the development of more effective adsorbent materials, which is a major focus of current research related to environmental and industrial applications (Gupta et al., 2009; Crini, 2006).

3. Results and discussion

3.1. Visual representation of adsorbent details before and after the adsorption process

Figure 2 shows a visual comparison of CW adsorbent granules before and after the adsorption process from textile waste. Changes in texture and color in granules after adsorption indicate CW's ability to absorb solute substances, including organic and inorganic compounds. This provides visual evidence that CW adsorbents, which are derived from carbide waste, are effective in removing color and lowering COD from textile wastewater.

3.2. Study of CW characteristics

The structural characteristics of CW adsorbent particles were evaluated before and after application in the adsorption process of Jumputan fabric waste. The morphology and texture

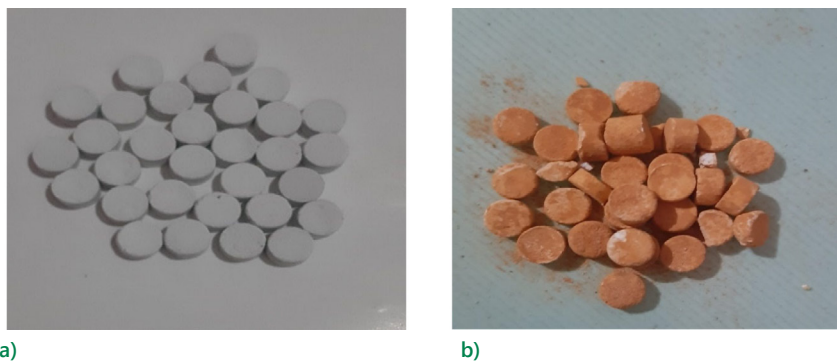


Figure 2. Visual comparison of adsorbent granules: a) before; b) after the adsorption process

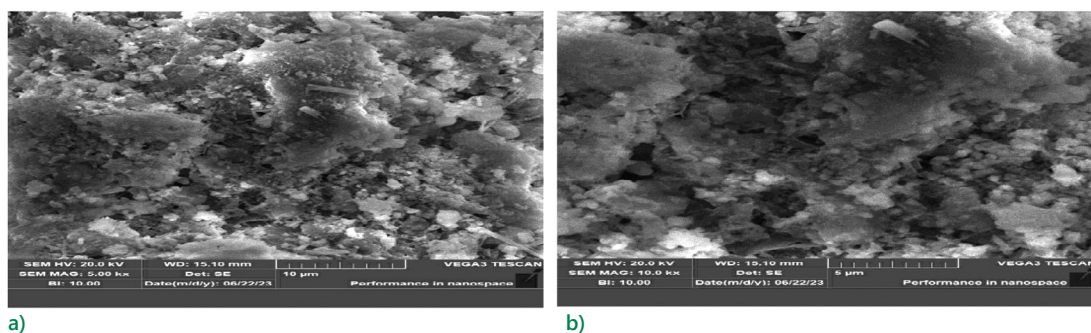


Figure 3. SEM image of carbide waste surface morphology: a) before adsorption; b) after adsorption at 5000x magnification

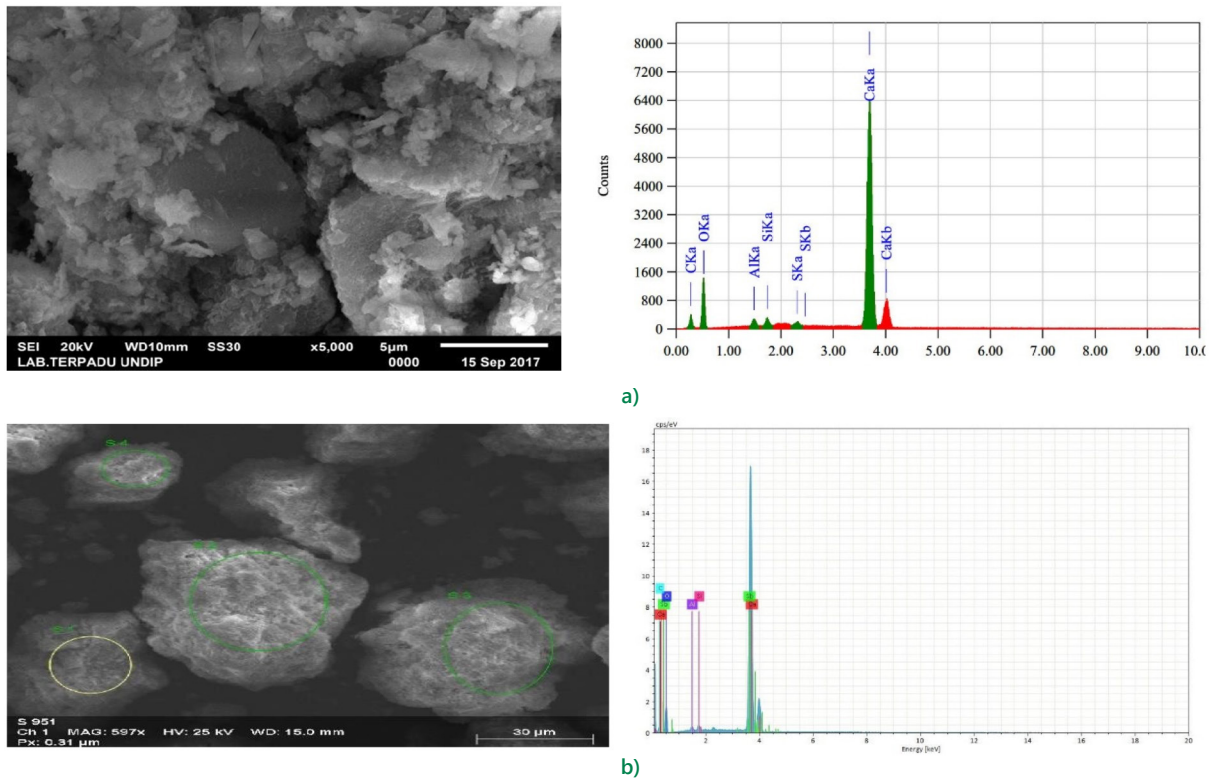


Figure 4. SEM-EDX analysis results: a) before adsorption; b) after adsorption process

of CW adsorbent particles were analyzed using Scanning Electron Microscopy (SEM) at a magnification of 5000x. The results of the SEM analysis are presented in Figure 3.

Figure 2 shows the initial morphology of the CW adsorbent surface before contact with Jumputan fabric waste. The SEM scanning results reveal the presence of abundant cavities and pores, indicating the potential of CW to absorb color and COD from the Jumputan fabric waste. Figure 1b depicts the surface morphology of the CW adsorbent after exposure to the Jumputan fabric waste. The structure observed in the image shows a solid formation with fused crystals, indicating significant changes on the adsorbent surface following the adsorption process. The presence of visible pores confirms that adsorption has occurred on the adsorbent surface.

SEM-EDX analysis before and after the adsorption process provides essential information regarding the physical and chemical characteristics of the adsorbent and adsorbate. This information is crucial for understanding the adsorption mechanism, evaluating process efficiency, and optimizing operating conditions for practical applications in waste treatment or water purification. The EDX analysis before and after the adsorption process is presented as shown in Figure 4.

In SEM Figure 2a, it can be observed that the surface morphology before the adsorption process exhibits a relatively smooth structure with clearly visible pores. This indicates that the adsorbent possesses a well-suited structure for the adsorption process due to its large surface area, allowing for effective contact with the adsorbate. The

elemental composition obtained from the EDX analysis reveals that the main components of this adsorbent are calcium (Ca), oxygen (O), and carbon (C), with atomic percentages of 56.84%, 26.19%, and 13.84%, respectively. Other elements such as aluminum (Al), silicon (Si), and sulfur (S) were also detected in smaller amounts, as shown in Table 1.

Table 1. Composition of carbide waste adsorbents before and after the adsorption process

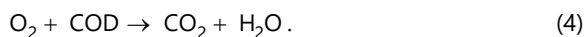
No	Pre-adsorption process		Post adsorption process
	Combination	% atom	% atom
1	Calcium	56.84	40.44
2	Antimony	–	31.92
3	Oxygen	26.19	22.69
4	Karbon	13.84	3.85
5	Aluminum	1.260	0.71
6	Silicon	1.220	0.60
7	Sulfur	0.650	–
	Total	100	100

In SEM Figure 3b, the surface morphology of CW after the adsorption process shows significant changes in the adsorbent's surface structure. The surface becomes rougher, with indications of adsorbate particle accumulation, confirming that the adsorption process has occurred. Some pores appear to be more occluded by the bound adsorbate. The elemental composition measured through EDX shows changes after adsorption, as presented in Table 1. Calcium

(Ca) decreased from 56.84% to 40.44%. Carbon (C) also showed a significant decrease from 13.84% to 3.85%, while oxygen (O) slightly decreased from 26.19% to 22.69%. Conversely, antimony (Sb), which was not detected before the adsorption process, appeared with a percentage of 31.92%, indicating that antimony has been adsorbed onto the adsorbent's surface. This antimony is suspected to originate from the catalysts used in the dyeing process of synthetic fibers contained in the Jumputan fabric wastewater.

According to Biver (2021), antimony is released from fibers during the dyeing process at high temperatures and subsequently discharged along with wastewater into rivers. It has been observed that up to 175 ppm of antimony can be released from fibers during the dyeing process. This data indicates that carbide waste adsorbent is capable of absorbing the colorants contained in Jumputan fabric wastewater.

The reduction in oxygen content from 26.19% to 22.69% suggests that oxygen has been consumed during the adsorption process, which potentially increases dissolved oxygen levels in water and lowers COD values. This can be assumed to occur through oxygen degradation reactions as follows:



3.3. Adsorbent characterization using FTIR analysis

Functional group characterization of the adsorbent was performed using FTIR spectroscopy to identify the functional groups present in the material. A mid-infrared

spectrophotometer with a wavenumber range of 400–4000 cm^{-1} was used for this analysis. FTIR generated a transmittance spectrum (%) that displayed absorption peaks at various wavelengths. The FTIR analysis results for the adsorbent are presented in Figure 5.

Figure 5 shows absorption peaks with high intensity centered at 3635.71 cm^{-1} and 2512.50 cm^{-1} , corresponding to OH groups, indicating the presence of strong hydrogen bonds from carboxylates. Additionally, strong and sharp absorptions associated with CH functional groups are observed at wavelengths of 1407.23 cm^{-1} , 869.30 cm^{-1} , 958.24 cm^{-1} , 734.46 cm^{-1} , and 702.18 cm^{-1} . At the wavelength of 1640.34 cm^{-1} , a variable absorption was identified, corresponding to the C = C functional group in alkenes. The wavelength of 1106.71 cm^{-1} shows a sharp absorption related to the CO functional group in alcohols. These results indicate the presence of a significant number of hydroxyl and oxygen groups on the surface of carbide waste, enabling the carbide waste to adsorb substances quickly and efficiently.

3.4. Adsorption experiments

3.4.1. Effect of contact time

The efficiency of COD reduction and color removal from Jumputan textile wastewater using CW adsorbent is illustrated in Figures 6a and 6b. Figure 6a shows the decrease in COD concentration in the Jumputan fabric wastewater. The percentage reduction in COD gradually increased from 30 to 150 minutes, then reached a stable point between

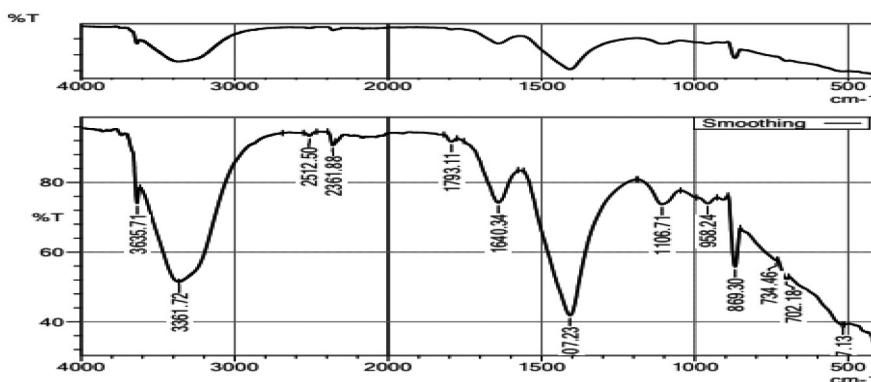


Figure 5. FTIR spectrum of carbide waste adsorbent after contact with textile waste

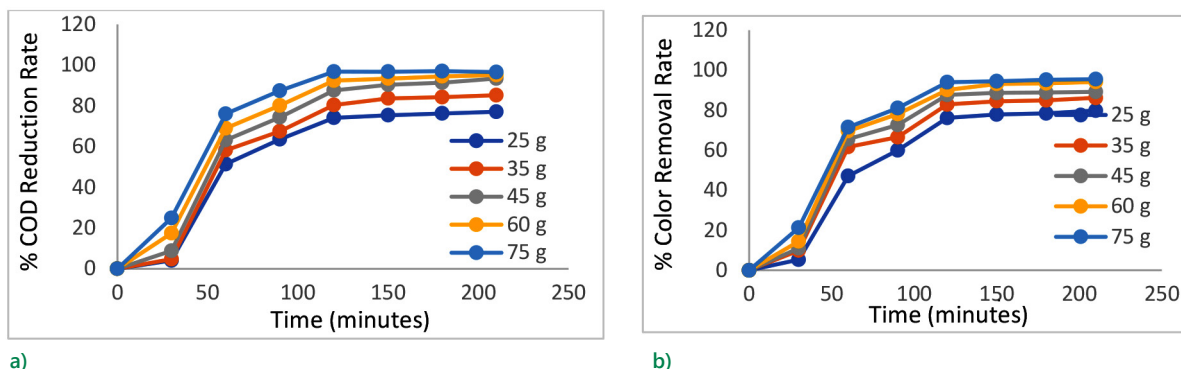


Figure 6. Effect of contact time of carbide waste on efficiency: a) rate of COD reduction; b) rate of color removal

150 and 210 minutes, indicating the occurrence of saturation. The effectiveness of COD reduction in Jumputan fabric wastewater also increased with the increasing mass of the adsorbent.

At an adsorbent mass of 7.5 g, COD reduction began to be observed at 30 minutes, with a decrease of 24.87%, and continued to increase until reaching 96.77% at 120 minutes. Subsequently, the percentage reduction in COD approached stability between 150 and 210 minutes, with a slight decrease in the reduction percentage to 95.52%. This indicates that the adsorbent reached its saturation point during this period, where no more available space remained to absorb additional substances from the solution. At this point, the adsorbent could no longer adsorb additional additives with significant efficiency, and the adsorption process had reached equilibrium. Thus, the CW adsorbent achieved equilibrium in reducing the COD concentration of Jumputan textile wastewater between 120 and 210 minutes, specifically at 150 minutes.

Figure 6b illustrates that the rate of color removal increases over time. The removal of color using 7.5 g of CW adsorbent began to be observed at 30 minutes, with a removal percentage of 21.29%. This percentage continued to increase, reaching 93.99% at 120 minutes. After that, from 150 to 210 minutes, the color removal percentage remained nearly stable at 94.48%, indicating that the adsorbent had reached the saturation phase. Therefore, it can be concluded that maximum color removal was achieved at 120 minutes with 7.5 g of carbide waste adsorbent.

The correlation between the amount of adsorbent and the degree of color change becomes evident through SEM-EDX analysis results, which show the presence of 31.92% antimony content. Additionally, FTIR analysis revealed the presence of CH functional groups, characterized by strong and sharp absorptions, which contribute to the effective absorption of dissolved substances.

3.4.2. Overview of the effect of solution pH

The acidity level of the solution has a significant impact on the removal of color and the reduction of COD contained in Jumputan fabric wastewater. To determine the elimination of color and the reduction of COD in Jumputan textile wastewater, pH variations ranging from 1 to 12 were

conducted, using 7.5 g of CW adsorbent per liter of textile wastewater, with a contact duration of 220 minutes, as shown in Figure 7.

The efficiency of dye removal shows a significant increase, particularly under acidic conditions, and stabilizes as the pH shifts towards the alkaline range. In Figure 7, it is evident that the percentage reduction in COD and the enhancement in textile dye removal reach their peak values at pH levels between 2 and 6. This indicates that the optimal pH for the adsorbent used is around pH 6, where the effectiveness of dye removal and COD reduction begins to stabilize and approaches its maximum value.

The optimal pH is the pH value at which the adsorbent surface has a net zero charge, influencing the electrostatic interactions between the adsorbent and the adsorbate. For the carbide waste adsorbent used in this study, the optimal pH was determined through the acid-base titration method and was found to be around pH 6. At pH levels below the optimal pH, the adsorbent surface carries a positive charge, enhancing electrostatic interactions with negatively charged dye ions, thereby increasing adsorption efficiency. Conversely, at pH levels above the optimal pH, the adsorbent surface becomes negatively charged, which increases the adsorption of positively charged dye ions until equilibrium is reached.

Research by El Haddad et al. (2012) indicates that dye adsorption is highly dependent on pH, with maximum adsorption occurring at around pH 6. Two possible adsorption mechanisms are electrostatic interactions between the surface groups of carbide waste and the functional groups of dye molecules, as well as chemical reactions between the carbide waste and dye molecules. At low pH, many adsorption sites on the adsorbent surface are occupied by protons, reducing the number of dye ions that can be absorbed due to the electrical repulsion between the adsorbent and protons. As the pH increases, the adsorbent surface becomes more negatively charged, enhancing the adsorption of positively charged dye ions until equilibrium is reached (Vimala & Das, 2009). This phenomenon also affects the ionization level of the adsorbate during the adsorption process, allowing the transfer of positive ions to the active sites of the adsorbent (Kilic et al., 2011).

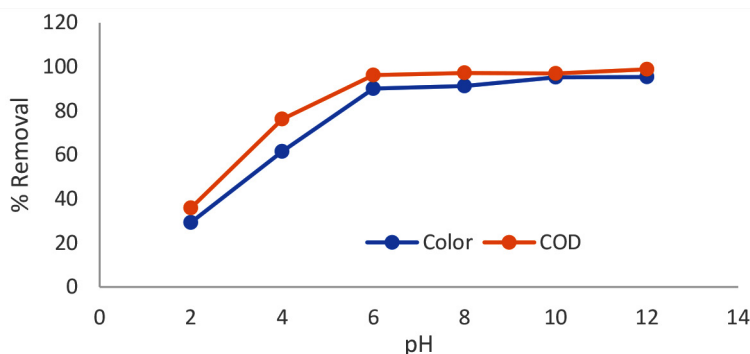


Figure 7. Impact of pH on COD and dye reduction

3.4.3. Effect of adsorbent quantity

The impact of varying the amount of CW adsorbent on the removal of color and reduction of COD in Jumputan textile wastewater was studied across different dosage spectrums: 2.5 g, 3.5 g, 4.5 g, 6.0 g, and 7.5 g. The initial wastewater concentrations were 34.589 mg COD/L and 45.591 Pt.Co. This study was conducted at ambient temperature (30 °C) over 150 minutes. The findings regarding color removal and COD reduction are presented in Table 2.

Table 2. Efficiency of color and COD removal and adsorption capacity at various doses of carbide waste adsorbent

Doses (g)	Color efficiency (% R)	COD efficiency (% R)	Color adsorption capacity (mg/g)	COD adsorption capacity (mg/g)	Standard deviation of color (mg/g)	Standard deviation COD (mg/g)
2.5	77.859	75.345	1.419	1.042	0.334	0.234
3.5	84.499	83.616	1.101	0.826		
4.5	88.675	90.352	0.898	0.695		
6	93.143	93.371	0.708	0.548		
7.5	94.479	96.730	0.574	0.446		

From Table 2 above, graphs illustrating the relationship between adsorbent mass and the removal efficiency and adsorption capacity for both COD and color were created, as depicted in Figure 6.

Figure 8 shows that increasing the dose of carbide waste adsorbent significantly enhances the efficiency of color and COD removal from textile wastewater. At a dose of 25 g, the color removal efficiency was recorded at 77.859%, while at a dose of 75 g, the efficiency increased to 94.479%. Similarly, COD removal efficiency increased from 75.345% at a dose of 25 g to 96.730% at a dose of 75 g. This indicates that increasing the adsorbent dose can improve the system's performance in removing pollutants from textile wastewater. However, this increase in dose is also accompanied by a decrease in adsorption capacity per unit mass of the adsorbent. The adsorption capacity for color decreased from 1419 mg/g at a dose of 25 g to 0.574 mg/g at a dose of 75 g. Similarly, the

adsorption capacity for COD decreased from 1042 mg/g to 0.4461 mg/g at the same dose. This decrease suggests that while more pollutants can be removed overall, the efficiency of adsorbent usage per gram diminishes with increasing doses. The recorded standard deviation for color adsorption capacity was 0.334 mg/g, and for COD adsorption capacity, it was 0.234 mg/g, indicating that the variability in these results is quite small and consistent. A similar study by Biswas et al. (2023) using a batch method also showed that increasing the adsorbent dose from 0.03 g to 0.3 g led to an increase in COD removal efficiency up to 87.4%. However, a decline in adsorption capacity per unit mass occurred after a certain dose, as indicated by the decrease in removal efficiency at higher doses. Furthermore, another study using the Fenton and UV/H₂O₂ processes for textile wastewater treatment also found that although increasing the adsorbent dose can enhance the efficiency of color and COD removal, there is a decrease in adsorption capacity per gram of adsorbent at higher doses (de Almeida et al., 2021).

3.4.4. Standard deviation analysis

Standard deviation analysis is a crucial statistical tool for understanding the spread and variability of data within a dataset. Here are some of the primary benefits of performing standard deviation analysis. Standard deviation can be used to evaluate the performance of a system or process. In experiments involving the removal of color and COD from textile wastewater, the standard deviation of removal efficiency can indicate how consistent the process is. A standard deviation analysis was performed based on Table 2, as shown in Table 3.

Table 3. Statistics of adsorbent mass, removal efficiency, adsorption capacity, and standard deviation

Parameter	Average	Deviation	Median
Massa Adsorbent (g)	4.8	19.87	4.50
Efficiency Warna % R	87.731	67.7530	88.675
Efficiency COD % R	87.8828	85.1311	90.352
Adsorption Capacity (q_e) of Color (mg/g)	940.0	0.33351	0.898
Adsorption Capacity (q_e) of COD (mg/g)	711.4	0.23443	0.695

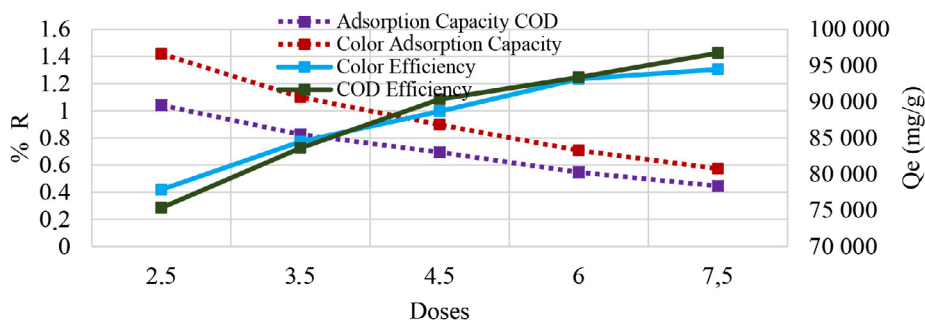


Figure 8. Adsorption capacity of COD and color at various doses of carbide waste adsorbent

From Table 3, it can be seen that the average adsorbent mass is 4.8 grams with a standard deviation of 19.87 grams and a median value of 4.50 grams. The relatively small standard deviation indicates that the adsorbent mass used in the experiments did not exhibit significant variation. This suggests that the use of adsorbent mass was consistent across the trials.

The color removal efficiency (% R) has an average of 87.731% with a standard deviation of 67.7530% and a median of 88.675%. The average COD removal efficiency (% R) is 87.8828% with a standard deviation of 85.1311% and a median value of 90.352%. The average adsorption capacity for color (q_e) is 0.940 mg/g with a standard deviation of 0.33351 mg/g and a median value of 0.898 mg/g. The average adsorption capacity for COD (q_e) is 0.711 mg/g with a standard deviation of 0.23443 mg/g and a median value of 0.695 mg/g.

From this statistical analysis, it can be concluded that although there is substantial variability in the removal efficiency (% R) for both color and COD, the adsorption capacity (q_e) for these parameters shows good consistency. This indicates that while removal efficiency may be influenced by various external factors, the fundamental ability of the adsorbent to absorb contaminants remains stable. Therefore, calcium carbide waste adsorbent can be considered a reliable option for the removal of color and COD from textile wastewater.

3.4.5. Effect of temperature

This study evaluated the effect of temperature on the efficiency of COD and color removal from textile wastewater using calcium carbide waste adsorbent. The tests were conducted at temperatures ranging from 30 °C to 45 °C, with an initial COD concentration of 34.589 mg/L and a color concentration of 4.559 Pt/Co, at pH 6, an adsorbent dose of 75 g, and a contact time of 150 minutes.

Figures 9a and 9b show variations in COD and color removal percentages over a temperature range of 30–45 °C. The linear equation obtained from the image was used to analyze the effect of temperature on the COD removal percentage, color removal, adsorption rate, and standard

deviation in textile wastewater. The calculated standard deviation values are summarized in Table 4, which provides a more detailed picture of the variability of adsorption performance and facilitates the comparative analysis of the two parameters.

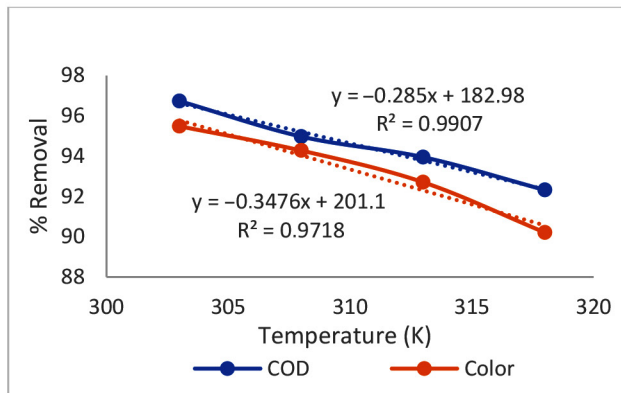
The data in Table 4 shows that increasing the temperature leads to a decrease in COD removal efficiency from 96.73% at 30°C to 92.32% at 45 °C, as well as a reduction in color removal from 95.48% to 90.21% (expressed in Pt/Co). This decline indicates the exothermic nature of the adsorption process, where increased temperature raises the kinetic energy of the adsorbate molecules, leading to desorption.

Table 4. Effect of temperature on COD and color removal percentage, adsorption rate, and standard deviation in textile wastewater

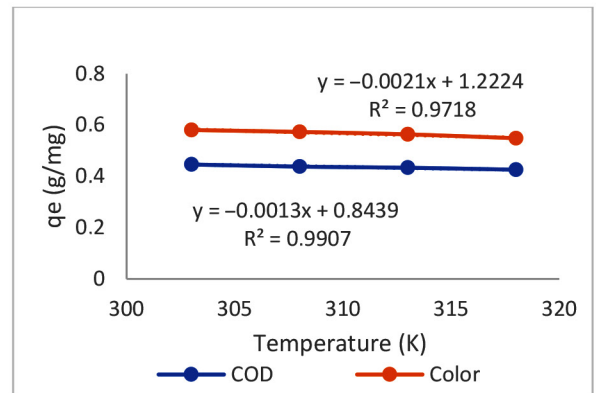
Temperature (°C)	COD removal percentage (% R)	Adsorption rate COD (mg/g-min)	Color removal percentage (% R)	Color adsorption rate (TCU/g-min)	Standard deviation COD	Standard deviation Warna
30	96.73	0.446	95.48	0.580	1.85%	2.28%
35	94.97	0.438	94.28	0.573	1.85%	2.28%
40	93.45	0.433	92.71	0.564	1.85%	2.28%
45	92.32	0.426	90.21	0.548	1.85%	2.28%

This phenomenon is consistent with previous reports by Kose and Kivanc (2011) and Zhang et al. (2019), who also noted a decrease in adsorption efficiency with increasing temperature. Additionally, the COD adsorption rate decreased from 0.446 mg/g-min at 30 °C to 0.426 mg/g-min at 45 °C, while the color adsorption rate decreased from 0.580 Pt/Co/g-min to 0.548 Pt/Co/g-min. The standard deviation for COD removal was 1.85%, and for color removal, it was 2.28%, indicating small and acceptable variations within the context of this experiment.

These findings are also in line with the study by Gupta et al. (2011), which reported a decrease in methylene blue



a)



b)

Figure 9. Effect of temperature on adsorption efficiency: a) percentage of color and COD removal; b) adsorption rate for color and COD

adsorption capacity on nano-cupric oxide with increasing temperature, as well as the results of Senthilkumar et al. (2006), which indicated that the optimal temperature for the adsorption of organic pollutants is between 25–35 °C. Therefore, lower temperatures are more effective in the adsorption process for the removal of COD and color from textile wastewater, confirming the exothermic character of this process.

3.4.6. Desorption and regeneration efficiency

The following figure presents the desorption and regeneration efficiency data of calcium CW after four regeneration cycles. The graph illustrates how desorption and regeneration efficiencies change with an increasing number of cycles, providing insights into the stability and sustainability of using CW as an adsorbent in long-term applications. This data is crucial for understanding the performance of CW material in maintaining its adsorption capacity after multiple uses and regenerations.

Figure 10 illustrates the desorption and regeneration efficiencies of calcium CW as an adsorbent over four regeneration cycles. The graph shows that desorption efficiency gradually decreases from 97% in the first cycle to 90% in the fourth cycle. Regeneration efficiency also exhibits a moderate decline, from 94% in the first cycle to 88% in the fourth cycle. This slower decline indicates that CW has good stability as an adsorbent across multiple regeneration cycles, maintaining relatively high performance. In contrast, a study by Momina et al. (2020) reported that bentonite exhibited a more significant efficiency drop after several regeneration cycles (desorption efficiency decreased to 70% after seven cycles). CW demonstrates superior stability in regeneration, suggesting that CW may be a better alternative to bentonite for long-term applications, especially in the context of adsorbent regeneration.

3.4.7. Langmuir isotherm model

In this study, the Langmuir and Freundlich isotherm models were used to model the adsorption process. The Langmuir isotherm model describes monolayer adsorption, assuming that all adsorption sites have a uniform affinity for

the adsorbate. This means that each molecule adsorbed on the surface has the same adsorption activation energy, leading to the formation of a single layer (monolayer).

It is important to note that the Langmuir isotherm equation explains surface coverage by balancing the rates of adsorption and desorption, also known as dynamic equilibrium. Adsorption is associated with the fraction of available open surface area, while desorption is related to the fraction of surface area that has been covered (Gunay et al., 2007). The Langmuir equation is represented by the following Equation (5) (Vunain et al., 2013):

$$\frac{C_e}{q_e} = \frac{1}{Q_m K_L} + \frac{1}{Q_m}, \quad (5)$$

where q_e represents the equilibrium adsorption capacity of COD and color (mg/g), C_e represents the equilibrium concentration of color and COD in the solution (mg/L), Q_m represents the maximum adsorption capacity (mg/g), and K_L is the Langmuir isotherm constant (L/mg), which describes the affinity of the adsorbent for the adsorbate. The value of R_L , which indicates the suitability of the Langmuir isotherm model for the adsorption process, can be calculated using Equation (6) as follows (Garba & Rahim, 2016; Vunain et al., 2013):

$$R_L = \frac{1}{(1 + C \cdot K_L)}. \quad (6)$$

It is important to note that the value of R_L provides insights into the adsorption behavior characteristics according to the Langmuir model. If $R_L < 1$, it indicates that adsorption is favorable (strong adsorption). A value of $R_L = 1$ indicates that adsorption does not alter the initial concentration of the solute. Conversely, if $R_L > 1$, it suggests that adsorption is less effective (weak adsorption).

3.4.8. Freundlich isotherm model

The Freundlich isotherm model differs from the Langmuir isotherm model as it does not assume the formation of a single layer of adsorbate on the adsorbent surface. Instead, this model provides a description that accounts for surface heterogeneity and the exponential distribution of

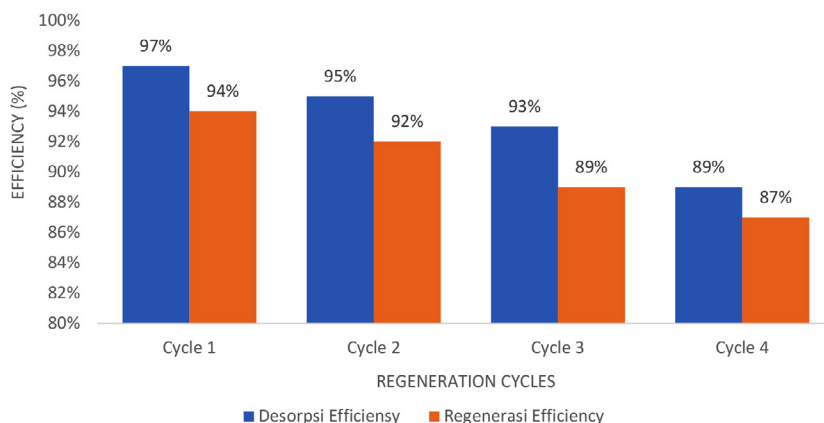


Figure 10. Desorption and regeneration efficiency of calcium carbide waste (CW) Over 4 regeneration cycles

active sites and their adsorption energies. The Freundlich isotherm suggests that the adsorption process occurs on a heterogeneous surface, where the availability of active sites with varying adsorption energies is unevenly distributed (Ayawei et al., 2015). Thus, the adsorbent surface is considered heterogeneous. The linear form of the Freundlich isotherm equation is expressed as follows Equation (7) (Boparai et al., 2011):

$$\ln q_e = \ln K_F + \frac{1}{n} (\ln C_e), \tag{7}$$

where q_e represents the amount of adsorbate at equilibrium (mg/g), C_e is the concentration of dye and COD in the solution at equilibrium (mg/L), K_F indicates the adsorption capacity, and n represents the adsorption intensity according to the characteristics described by the Freundlich constant.

The data obtained in this experiment under equilibrium conditions were analyzed using the Langmuir and Freundlich isotherm models to assess the adsorption performance of carbide waste for color removal and COD reduction. The analysis data for color removal and COD reduction with initial concentrations of 45.591 Pt.Co for color and 34.589 mg/L for COD at an equilibrium time of 150 minutes are presented in Table 4.

From the data obtained and listed in Table 5, it is evident that increasing the adsorbent dosage consistently enhances the percentage of color and COD removal. At a dosage of 2.5 g, color removal reached 77.86%, and COD removal was 75.34%. These percentages continued to increase, reaching

94.48% for color and 96.73% for COD at the highest dosage of 7.5 g. This indicates that increasing the adsorbent dosage significantly improves adsorption capacity, which aligns with the theory that more active sites are available for the adsorption process at higher dosages.

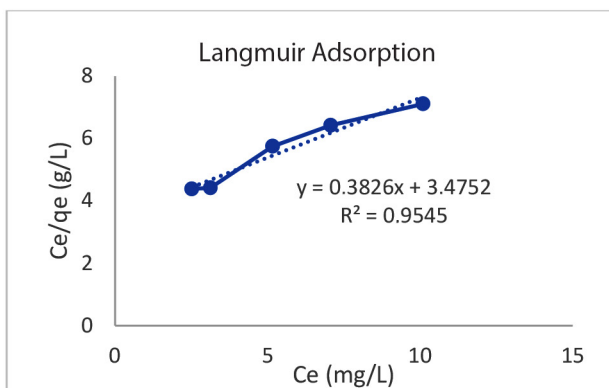
Based on the available table, graphs were generated depicting the relationship between q_e and C_e for each isotherm model, including the Langmuir and Freundlich isotherm models. The analysis of the adsorption process for color removal and COD reduction was conducted by correlating the experimental data from the batch equilibrium study, as illustrated in Figures 11a and 11b.

From the calculations based on Figures 11a, 11b and 12a, 12b, the Langmuir and Freundlich parameters, as well as the Sum of Squared Errors (SSE) for color adsorption, were obtained as listed in the table. The calculated parameters for both models are summarized in Table 6, which presents the parameter values obtained from the Langmuir and Freundlich models for color and COD.

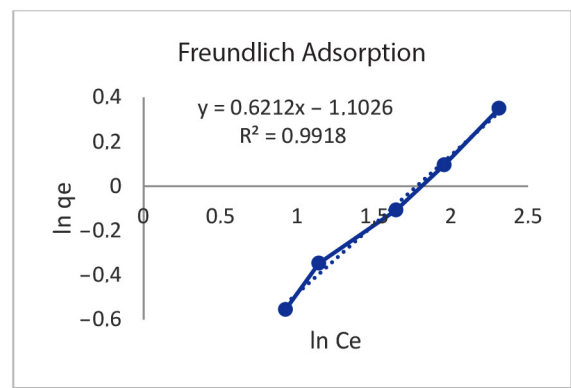
Based on the data in Table 6, it is observed that in the Langmuir model for color removal, the maximum adsorption capacity obtained is 0.288 mg/g, while for COD reduction, is 0.449 mg/g. The Langmuir constant (K_L), which indicates the affinity of the adsorbent for the adsorbate, is recorded at 9.083 L/mg for color and 3.05 L/mg for COD. The very small separation factor (R_L) values, 0.002 for color and 0.009 for COD indicate that the adsorption process is highly favorable under the tested conditions. The determination coefficient shows a good fit between the model and the experimental data, with values of 0.955

Table 5. Adsorption isotherm data analysis

Doses (g)	C_0 (Color) Pt.Co	C_0 (COD) (mg/L)	C_e (Color) Pt.Co	C_e (COD) (mg/L)	% R Color	% R COD	q_e Color	q_e COD
2.5	45.591	34.589	10.094	8.528	77.859	75.345	0.1419	0.1042
3.5	45.591	34.589	7.067	5.667	84.499	83.616	0.1101	0.0826
4.5	45.591	34.589	5.164	3.337	88.673	90.352	0.0898	0.0695
6.0	45.591	34.589	3.126	2.293	93.143	93.371	0.0708	0.0538
7.5	45.591	34.589	2.517	1.131	94.479	96.730	0.0574	0.0446



a)



b)

Figure 11. Shows the adsorption isotherms for color removal: a) Langmuir; b) Freundlich

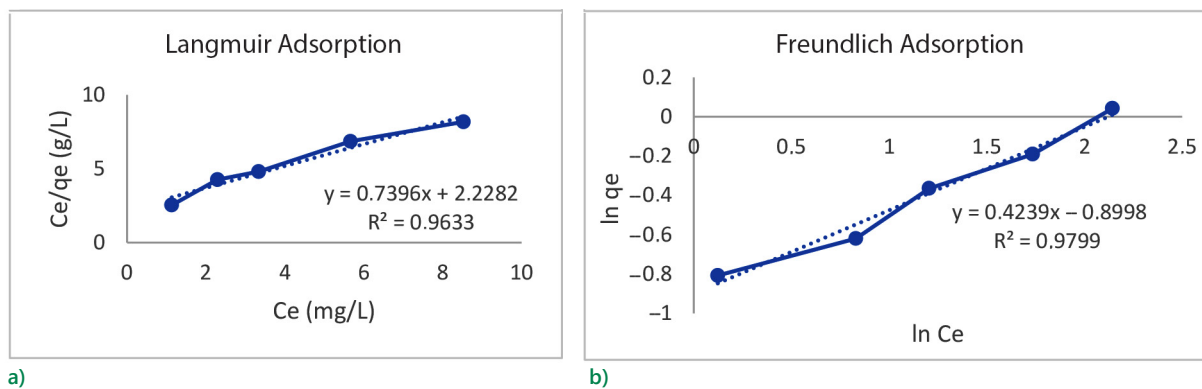


Figure 12. Shows the adsorption isotherms for COD removal: a) Langmuir; b) Freundlich

for color and 0.963 for COD. However, the relatively higher SSE values, 0.187 for color and 0.000645 for COD indicate some deviation between the model predictions and the experimental data.

Table 6. Adsorption isotherm parameters for the Langmuir and Freundlich models

Isotherm	Parameter	Color	COD
Langmuir	Line equation	$Y = 0.3826x + 3.4752$	$Y = 0.7396x + 2.2282$
		2.288	0.449
		9.083	3.05
		0.9545	0.9963
	SSE	0.002	0.009
Freundlich	Line equation	$Y = 0.6212x - 1.1026$	$Y = 0.4239x - 0.8998$
		0.079	0.126
	1/n	1.61	2.36
		0.9918	0.9799

On the other hand, the Freundlich model is used to describe adsorption on heterogeneous surfaces. The Freundlich constant (K_F), which represents adsorption capacity, is 0.079 (mg/g)(L/mg) for color and 0.126 (mg/g)(L/mg) for COD. The exponent n , which reflects the intensity of adsorption, is recorded as 1.61 for color and 2.36 for COD. The larger the n value, the more nonlinear the adsorption character, reflecting the heterogeneity of the adsorbent surface. The Freundlich model exhibits excellent determination coefficients (R^2), 0.992 for color and 0.98 for COD, indicating a high level of agreement between the model and the experimental data. The lower SSE values compared to the Langmuir model, 0.032 for color and 0.00705 for COD, suggest that the Freundlich model provides more accurate predictions of the experimental data.

Overall, both isotherm models are capable of effectively describing the adsorption process. However, the Freundlich model is more suitable for depicting this phenomenon, especially in conditions where the adsorbent surface is heterogeneous. The Freundlich model provides a higher R^2 values and lower SSE, indicating better accuracy

in predicting experimental results. Although the Langmuir model offers important parameters such as maximum adsorption capacity, in this context, the Freundlich model proves to be superior in describing the adsorption process on the CW adsorbent used. Bote et al. (2021) used carbon adsorbents derived from water filter cartridges (AC-EWFC), which showed excellent performance in removing blue methylene (MB) with a maximum adsorption capacity of 55.62 mg/g. The adsorption process follows the isothermal model of Langmuir and Freundlich, which shows that adsorption occurs in both monolayer and multilayer. In addition, adsorption also follows the second pseudo-order kinetics, reflecting the high efficiency in binding MB to the active surface of the adsorbent.

3.5. Temkin isotherm

The Temkin isotherm is an adsorption model that takes into account the interactions between the adsorbate and the adsorbent and assumes that the adsorption energy decreases linearly with increasing adsorbate coverage on the adsorbent surface. This differs from the Langmuir and Freundlich isotherms, which assume uniform and coverage-independent adsorption energy, respectively. The linear form of the Temkin equation can be given as follows in Equation (8) (Khatibi et al., 2022):

$$q_e = \frac{RT}{b} \ln(K_T C_e). \quad (8)$$

In its linear form, Equation (8) can be rewritten as Equation (9).

$$q_e = B \ln(C_e) + B \ln(K_T), \quad (9)$$

where q_e is the amount of substance adsorbed per unit weight of adsorbent at equilibrium (mg/g), C_e is the concentration of solute at equilibrium (mg/L), K_T is the Temkin constant (L/g).

$$B = \frac{RT}{b}, \quad (10)$$

where R is the gas constant (8.314 J/mol·K), T is the absolute temperature (K), b is the constant related to the variation in adsorption energy (J/mol).

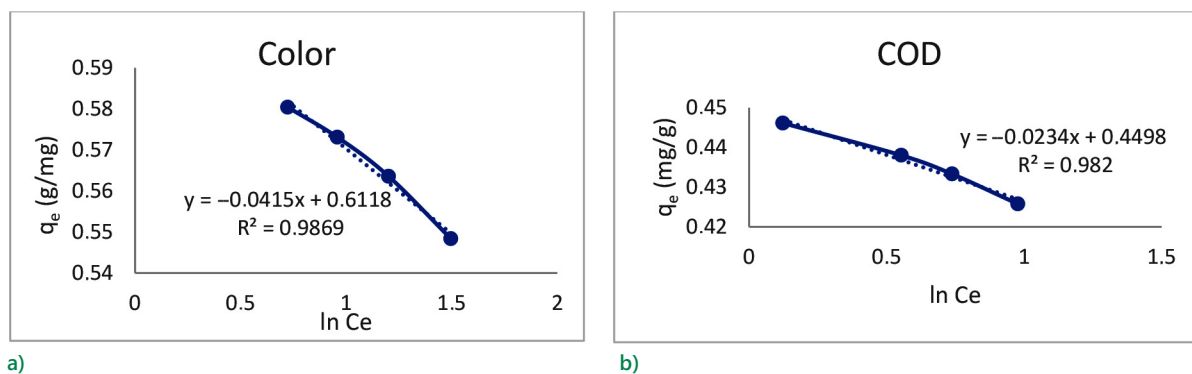


Figure 13. Illustrate the effect of temperature on Temkin parameters: a) for color removal; b) for COD removal

The Temkin isotherm is based on the assumption that the adsorption energy of all molecules in the layer decreases linearly with surface coverage due to adsorbate-adsorbent interactions. A plot of q_e vs. $\ln(C_e)$ is used to obtain the slope B and intercept $B \cdot \ln(K_T)$, as shown in Figures 4 and 5.

From Figures 13a and 13b, the line equations for COD ($y = -0.0234x + 0.4498$, $R^2 = 0.982$) and for Color ($y = -0.0415x + 0.6118$, $R^2 = 0.9869$) can be used to calculate the Temkin parameters and SSE, as shown in Table 5.

Table 7. Temkin isotherm parameters and SSE for COD and color

Temperature	COD			Color		
	B_T (J/mol)	K_T (L/g)	SSE	B_T (J/mol)	K_T (L/g)	SSE
303.15	107.725	1.0042	1.0×10^{-8}	60.725	1.0101	0.0
308.15	109.370	1.0041	1.0×10^{-8}	61.645	1.0101	0.0
313.15	111.015	1.0040	1.0×10^{-8}	62.565	1.0100	0.0
318.15	112.660	1.0039	1.0×10^{-8}	63.485	1.0099	0.0

From Table 7, it is observed that the parameter for COD and color increases with rising temperature, for example, from 107.725 J/mol at 303.15 K to 112.600 J/mol at 318.15 K for COD, and from 60.725 J/mol to 63.485 J/mol for color at the same temperatures. This increase in B_T indicates that the energy required for the adsorption process rises, suggesting stronger interactions between the adsorbate and adsorbent at higher temperatures. Based on the increase in B_T , this adsorption process tends to be endothermic.

The K_T (Temkin equilibrium constant) values for COD and color remain relatively constant and close to 1, indicating that changes in temperature within the tested range do not significantly impact the adsorbent's affinity for the adsorbate. This stability in K_T suggests that although the adsorption energy increases, the adsorbent's ability to attract adsorbate molecules does not change significantly with increasing temperature.

The very low SSE values for COD and color indicate an excellent fit between the Temkin isotherm model and the

experimental data, particularly for color, where the error is almost negligible. This confirms that the Temkin model accurately predicts the adsorption behavior for both parameters across the tested temperature range.

3.6. Dubinin-Radushkevich (D-R) isotherm

The Dubinin-Radushkevich (D-R) isotherm is an adsorption model used to understand the adsorption mechanism, whether it is physical or chemical in nature. This model not only describes the maximum adsorption capacity but also provides information about the pore energy of the adsorbent, which can be used to determine whether the adsorption process is physical or chemical. The equation assumes that the pore distribution in the adsorbent follows a Gaussian energy distribution (Dąbrowski, 2001). The Dubinin-Radushkevich (D-R) adsorption isotherm is represented as follows:

$$q_e = q_m \exp(-\beta \epsilon^2), \quad (11)$$

where q_e is the amount of adsorbate adsorbed per unit mass of adsorbent at equilibrium (mg/g), q_m is the maximum adsorption capacity (mg/g), β is the constant related to the adsorption energy (mol^2/kJ^2), ϵ is the Polanyi potential, calculated as:

$$\epsilon = RT \ln \left(1 + \frac{1}{C_e} \right), \quad (12)$$

where R is the gas constant (8.314 J/mol·K), T is the temperature in Kelvin, C_e is the equilibrium concentration of the adsorbate in the solution (mg/L).

This study analyzed the Dubinin-Radushkevich (D-R) isotherm parameters to model the adsorption process of COD and color from textile wastewater at various temperatures: 30 °C, 35 °C, 40 °C, and 45 °C. As presented in Table 8, the Polanyi potential (ϵ) was calculated for each temperature, with results ranging from 2.227 J/mol to 0.996 J/mol for COD and from 1.223 J/mol to 0.593 J/mol for color. These values indicate that the energy involved in the adsorption process is van der Waals energy, suggesting that the adsorption process is physical.

From the data in the Table 8, a graph can be created, and the Maximum Adsorption Capacity (q_m) and the

Table 8. Relationship of temperature with adsorption energy (ϵ) and $\ln(q_e)$

Temp (°C)	ϵ COD (J/mol)	ϵ Color (J/mol)	$\ln(q_e)$ COD	$\ln(q_e)$ Color
30.0	2.227	1.223	13.01	13.27
35.0	1.470	0.984	12.99	13.26
40.0	1.240	0.782	12.98	13.24
45.0	0.996	0.593	12.96	13.22

Table 9. Dubinin-Radushkevich (D-R) isotherm parameters

Temp (°C)	q_m COD (mg/g)	K COD (mol^2/J^2)	E COD (J/mol)	SSE COD	q_m Color (mg/g)	K Color (mol^2/J^2)	E Color (J/mol)	SSE Color
30.0	412,091	0.038	3.651	0.1	519,696	0.094	2.303	0.44
35.0	412,091	0.038	3.651	0.1	519,696	0.094	2.303	0.44
40.0	412,091	0.038	3.651	0.1	519,696	0.094	2.303	0.44
45.0	412,091	0.038	3.651	0.1	519,696	0.094	2.303	0.44

Isotherm Constant (K) can be calculated from the plot of $\ln(q_e)$ against epsilon (ϵ^2).

From the Figure 14, the Dubinin-Radushkevich (D-R) isotherm parameters were calculated, and the results are presented in the Table 9.

The data obtained from these measurements were used to calculate the Maximum Adsorption Capacity (q_m) and the Isotherm Constant (K) through the plot of $\ln(q_e)$ against epsilon (ϵ^2). The calculation results (Table 9) show that for COD, the q_m value is 412.091 mg/g with K of 0.0375 mol^2/J^2 . Meanwhile, for color, q_m is recorded at 519 696 mg/g with K of 0.0943 mol^2/J^2 . This high adsorption capacity indicates that the adsorbent has a strong ability to bind pollutants.

The Mean Adsorption Energy (E) obtained is 3.65 J/mol for COD and 2.30 J/mol for color. An E value lower than 8 kJ/mol for both adsorbates indicates that the adsorption process is physical in nature, with van der Waals forces dominating the interaction between the adsorbent and adsorbate.

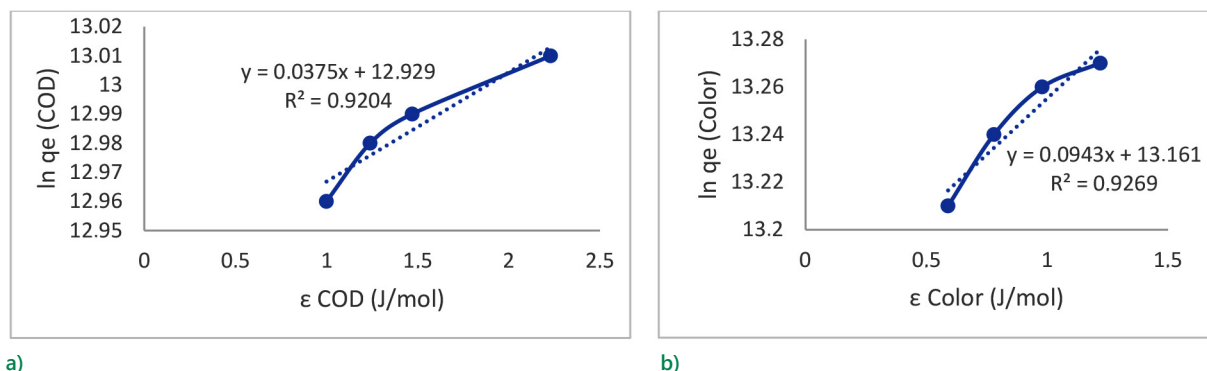
Additionally, a SSE analysis was conducted to evaluate the fit of the D-R isotherm model with the experimental data. The SSE values obtained were 0.1 for COD and 0.44 for color across the different temperatures tested. The low SSE values suggest that the D-R isotherm model has a good fit with the experimental data, reinforcing the

validity of the results obtained. The differences in q_m and K values between COD and color reflect the variations in the mechanism and strength of interactions between the adsorbent and each pollutant.

Furthermore, from the regression equations obtained, namely $y = 0.0375x + 12.929$ with $R^2 = 0.9204$ for COD and $y = 0.0943x + 13.161$ with $R^2 = 0.9269$ for color, it can be concluded that the D-R isotherm model has a very good correlation with the experimental data. The R^2 values close to 1 indicate that most of the variability in the data can be explained by this isotherm model, suggesting that this model is a fairly accurate representation of the adsorption process taking place.

3.7. Kinetic study

To understand the mechanisms governing the color removal and COD reduction process using CW adsorbent, various factors controlling the adsorption process must be considered, including pH, adsorbent mass, and contact time, as well as chemical reactions and mass transfer (Miler et al., 2016). The pseudo-first-order and pseudo-second-order Lagergren correlations were used to analyze the experimental data. The pseudo-first-order model is generally used to analyze adsorption data derived from the adsorption of adsorbates from aqueous solutions. This

**Figure 14.** Dubinin-Radushkevich (D-R) isotherm relationship on the absorption process: a) color; b) COD

model describes the adsorption rate as proportional to the number of available binding sites on the adsorbent (Hui et al., 2009). The pseudo-first-order Lagergren model, based on solid capacity, is usually expressed as follows (Cochrane et al., 2006):

$$\log(q_e - q_t) = \log q_e - \frac{K_1 t}{2.303}, \tag{13}$$

where q_e represents the amount of adsorbate absorbed onto the adsorbent at equilibrium, q_t denotes the amount of adsorbate absorbed onto the adsorbent at a specific time, and K_1 refers to the pseudo-first-order adsorption constant. The values of K_1 , K_2 and q_e can be determined from the graphical plot of $\log(q_e - q_t)$ versus t , where the slope and intercept of the linear graph are calculated (Gupta et al., 2012). The pseudo-second-order model, initially proposed by Taty-Costodes et al. (2003) and later discussed by Ho (2014), is expressed through the following Equation (14):

$$\frac{t}{q_t} = \frac{1}{k_2 q_e^2} + \frac{1}{q_e} t, \tag{14}$$

where k_2 represents the pseudo-second-order rate constant ($\text{g}\cdot\text{min}^{-1}\cdot\text{mg}^{-1}$). The values of k_2 and q_e can be determined from the intercept and slope of the linear plot of (t/q_t) versus t . This study evaluated the kinetics of color removal and Chemical Oxygen Demand (COD) reduction in textile wastewater using CW adsorbent with varying masses from 25 g to 75 g. Kinetic modeling was performed using both the first-order and second-order models to understand the dynamics of the adsorption process for each variation in adsorbent mass. The values of k_1 and q_e can be determined from the graphical plot of $\log(q_e - q_t)$ versus t , as well as the values of k_2 and q_e from the plot of (t/q_t) versus t , as shown in Figures 15–19.

To obtain the kinetic model parameters and SSE values for color removal and COD reduction, calculations

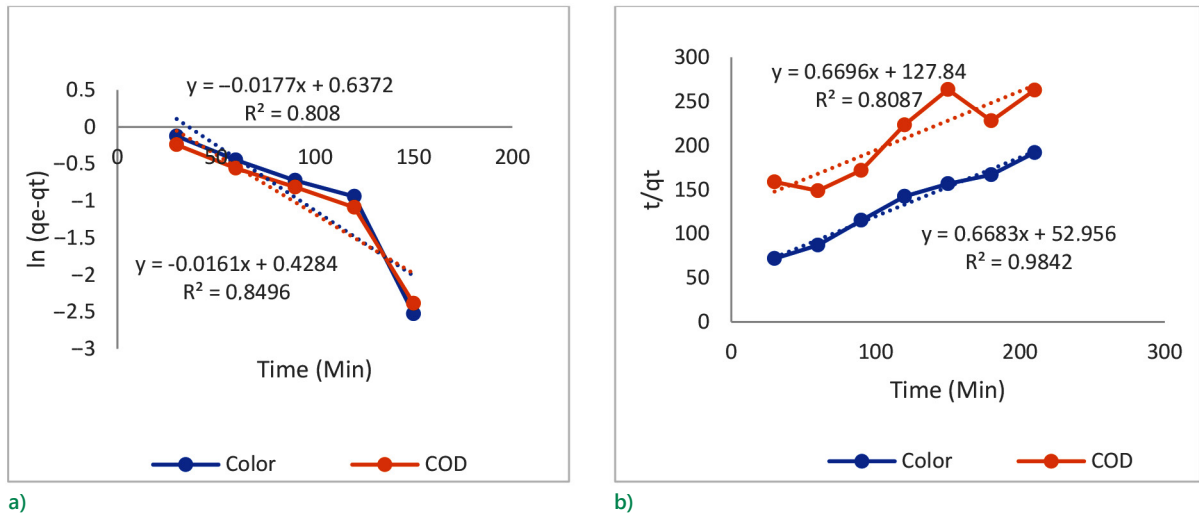


Figure 15. Kinetics of color removal and COD reduction with 2.5 g of carbide waste adsorbent: a) first-order modeling; b) second-order modeling

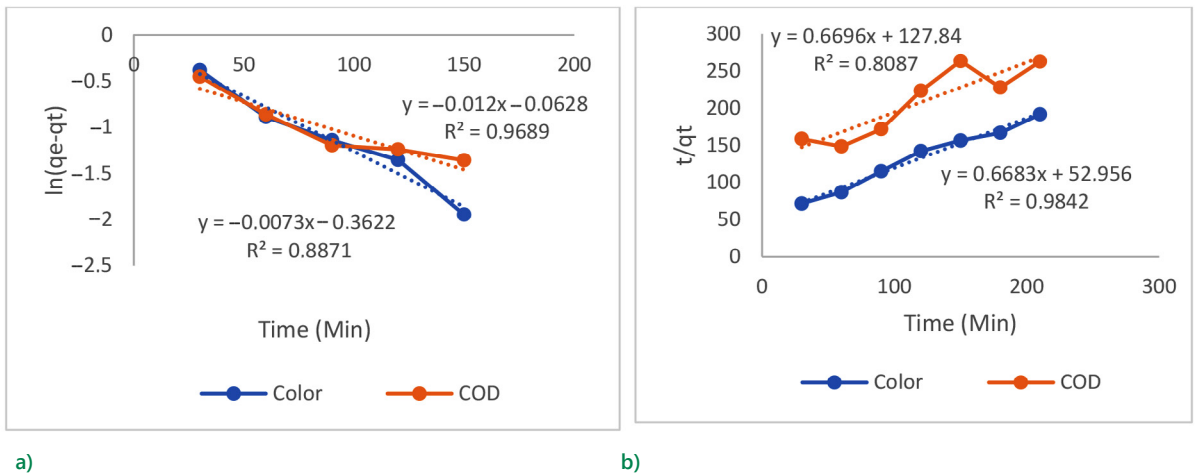


Figure 16. Kinetics of color removal and COD reduction with 3.5 g of carbide waste adsorbent: a) first-order modeling; b) second-order modeling

were performed using the line equations from Figures 10 to 14. The calculated values for first-order and second-order kinetic parameters are comprehensively presented in Tables 10 and 11.

The results in Tables 10 and 11 show that increasing the adsorbent mass affects the reaction rate and adsorption capacity. At a mass of 2.5 g, the reaction rate constant

(k_1) for color removal is 0.018 min^{-1} , with a theoretical adsorption capacity (q_e) of 0.529 mg/g (first-order) and 2.387 mg/g (second-order). At a mass of 7.5 g , k_1 increases to 0.046 min^{-1} , while is recorded at 0.589 mg/g (first-order) and 0.746 mg/g (second-order). The k_2 and SSE values indicate that the second-order model is more suitable for describing the adsorption kinetics.

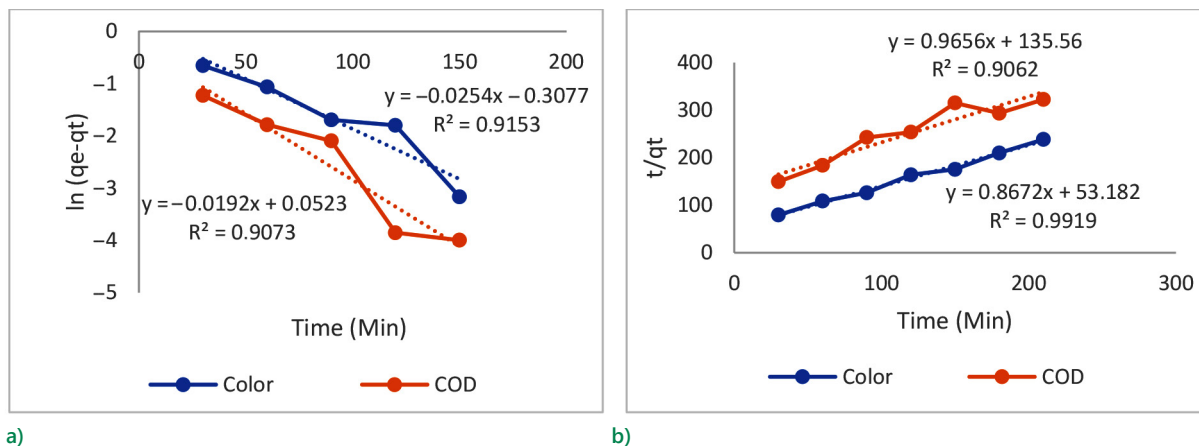


Figure 17. Kinetics of color removal and COD reduction with 4.5 g of carbide waste adsorbent: a) first-order modeling; b) second-order modeling

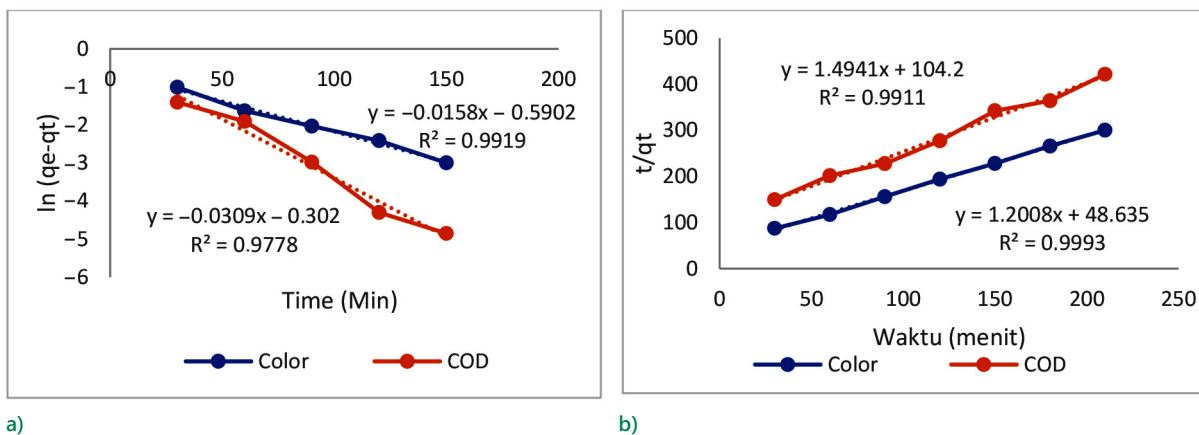


Figure 18. Kinetics of color removal and COD reduction with 6.0 g of carbide waste adsorbent: a) first-order modeling; b) second-order modeling

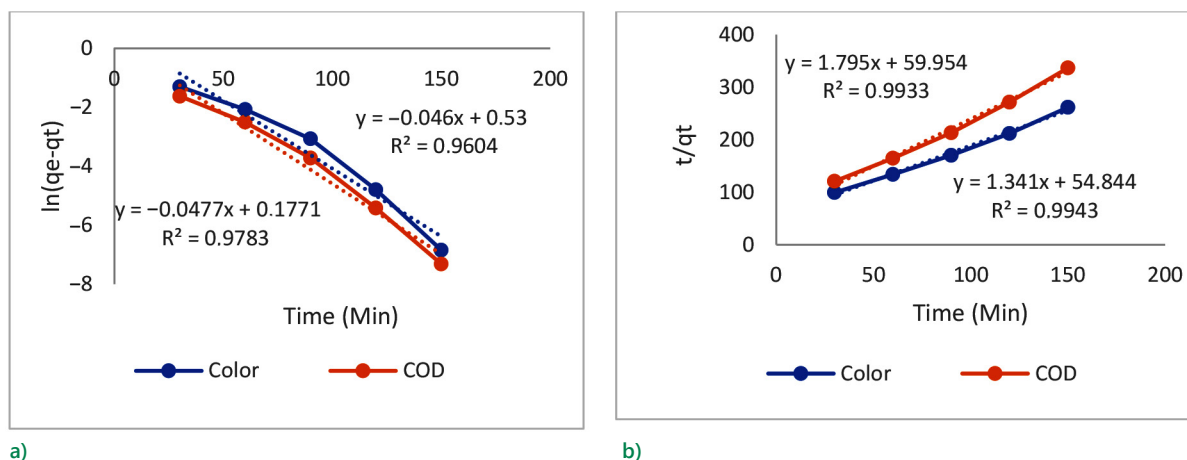


Figure 19. Kinetics of color removal and COD reduction with 7.5 g of carbide waste adsorbent: a) first-order modeling; b) second-order modeling

Table 10. Kinetic model parameters for color removal

Mass (gram)	Parameters of adsorption kinetics model								
	Pseudo-first-order equations				Pseudo-second-order equations				
	Line equations	q_e	k_1	R_2	Line equations	q_e	k_2	R_2	SSE
2.5	$Y = -0.017x - 0.64$	0.529	0.017	0.808	$Y = 0.419x + 106.21$	2.387	0.074	0.952	1.7035
3.5	$Y = -0.007x - 0.36$	0.696	0.007	0.887	$Y = 0.669x + 127.84$	1.493	0.3	0.984	1.4043
4.5	$Y = -0.025x - 0.308$	0.735	0.025	0.915	$Y = 0.867x + 53.182$	1.153	0.652	0.992	1.153
6.0	$Y = -0.016x - 0.590$	0.554	0.016	0.992	$Y = 1.201x + 48.635$	0.833	1.731	0.999	1.7215
7.5	$Y = -0.046x - 0.530$	0.589	0.046	0.960	$Y = 1.341x + 54.844$	0.746	2.411	0.994	1.153

Table 11. Kinetic model parameters for COD removal

Mass (gram)	Parameters of adsorption kinetics model								
	Pseudo-first-order equations				Pseudo-second-order equations				
	Line equations	q_e	k_1	R_2	Line equations	q_e	k_2	R_2	SSE
2.5	$Y = -0.016x + 0.428$	1.534	0.016	0.849	$Y = 0.455x + 49.719$	2.198	0.094	0.896	1.941
			0.012	0.969	$Y = 0.668x + 52.956$	1.497	0.298	0.809	1.941
4.5	$Y = -0.0192x - 0.05$	0.995	0.019	0.907	$Y = 0.966x + 135.56$	1.035	0.901	0.906	1.941
6.0	$Y = -0.0309x - 0.30$	0.97	0.031	0.979	$Y = 1.494x + 104.20$	0.669	3.335	0.991	1.941
7.5	$Y = -0.0477x - 0.18$	0.982	0.048	0.978	$Y = 1.795x + 59.950$	0.557	5.784	0.993	1.941

The COD reduction follows a similar pattern to color removal. At a mass of 2.5 g, k_1 for COD is 0.016 min^{-1} with q_e of 1.534 mg/g (first-order) and 2.198 mg/g (second-order). At a mass of 7.5 g, k_1 increases to 0.048 min^{-1} , but q_e decreases to 0.982 mg/g (first-order) and 0.557 mg/g (second-order). The second-order model, with better k_2 and SSE values are also more suitable for the COD reduction process. Overall, the second-order kinetic model is more accurate in describing the adsorption process for both color removal and COD reduction using CW adsorbent. The application of the pseudo-second-order kinetic model to the adsorption of color and COD reduction from Jumputan fabric wastewater onto the surface of CW adsorbent suggests that the adsorption process involves various mechanisms, including chemical interactions and electrostatic attraction of anions present in the Jumputan fabric wastewater to reactive sites on the surface of carbide waste (Taty-Costodes et al., 2003).

3.8. Intra-particle diffusion adsorption of color and COD

In this study, an analysis of color and COD adsorption in textile wastewater was conducted using carbide waste adsorbent. The intra-particle diffusion graph shown in Figure 20 provides insight into the mass transport process occurring during the adsorption. Based on the graph, it is evident that there is a relationship between contact time and the level of pollutant absorption, indicating the presence of an intra-particle diffusion mechanism.

From Figure 20 above, the intra-particle diffusion parameters can be calculated intra-particle diffusion parameters and the SSE related to the color adsorption and COD processes. Important parameters listed include the diffusion constant k_{diff} , intercept value (C), and SSE. This data provides insight into the effectiveness and complexity of the adsorption process for each parameter, namely color and COD.

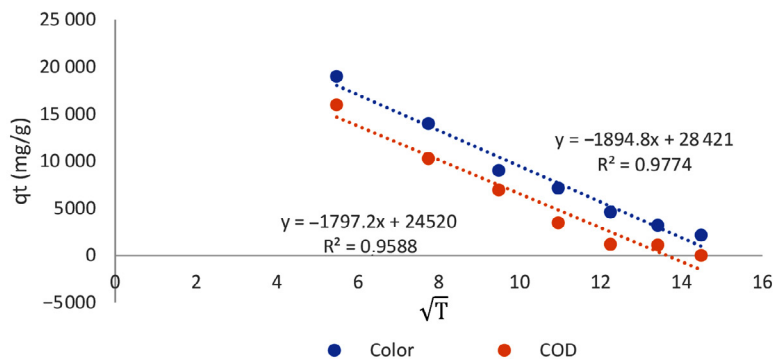


Figure 20. Intra-particle diffusion adsorption for color and COD in textile wastewater

Table 12. Intra-particle diffusion parameters and SSE

Parameters	Color	COD
k_{diff}	-1.895	-1.746
C	28.421	24.091
SSE	5.097	11.371

Table 12, this table helps in analyzing and comparing adsorption efficiencies for the two contaminants, as well as in understanding the mechanisms underlying the process. Diffusion and SSE parameters, relevant parameters such as diffusion constants k_{diff} , intercept values (C), and SSE for color adsorption and COD are listed. Based on the table, the (k_{diff}) value for color is -1.895, while for COD is -1.746. The intercept value (C) was higher for color (28.421) compared to COD (24.091). Meanwhile, the SSE value shows several square errors of 5.097 for color and 11.371 for COD. A higher SSE value for COD indicates that the COD adsorption process may be less efficient or more complex compared to color adsorption.

4. Conclusions

This study demonstrates that CW can be effectively utilized as an adsorbent for removing color and reducing COD from textile wastewater. At an adsorbent dose of 75 g, CW achieved a color removal efficiency of up to 94.48% and a COD reduction of 96.73%. The Freundlich isotherm model provided the best fit, with R^2 values of 0.9918 for color and 0.9799 for COD, along with low SSE values, indicating a good agreement with the experimental data.

The Temkin isotherm analysis revealed that adsorption energy increases with temperature, indicating the exothermic nature of the process. The low mean adsorption energy (E) values suggest that the adsorption process is dominated by van der Waals forces, characteristic of physical adsorption. The adsorption kinetics followed a pseudo-second-order model, indicating the presence of complex chemical interactions. Intra-particle diffusion analysis showed that mass transfer within the adsorbent particles plays a significant role in the adsorption process.

The reuse of CW adsorbent showed a decrease in color removal efficiency from 94.47% in the first cycle to 88% in the fourth cycle, while COD removal efficiency decreased from 96.73% to 90% in the fourth cycle. This suggests that the CW adsorbent becomes saturated after several cycles, highlighting the need for regeneration or replacement to maintain optimal performance in wastewater treatment. Overall, the findings of this study provide important insights into the potential of CW as an environmentally friendly and cost-effective solution for textile wastewater treatment, with implications for broader industrial applications.

References

- Adegoke, K. A., & Bello, O. S. (2015). Dye sequestration using agricultural wastes as adsorbents. *Water Resources and Industry*, 12, 8–24. <https://doi.org/10.1016/j.wri.2015.09.002>
- Ahmad, A. A., & Hamid, B. H. (2009). Reduction of COD and color from dye wastewater of a cotton textile mill through adsorption onto bamboo-based activated carbon. *Journal of Hazardous Materials*, 172(2–3), 1538–1543. <https://doi.org/10.1016/j.jhazmat.2009.08.025>
- Aichour, A., Djafer Khodja, H., & Zaghouane-Boudiaf, H. (2021). Removal of textile dyes from wastewater using promising novel composites: A review. *Algerian Journal of Chemical Engineering*, 2, 49–65.
- Almeida, C. A. P., Debacher, N. A., Downs, A. J., Cottet, L., & Mello, C. A. D. (2009). Removal of methylene blue from colored effluents by adsorption on montmorillonite clay. *Journal of Colloid and Interface Science*, 332(1), 46–53. <https://doi.org/10.1016/j.jcis.2008.12.012>
- Al-Musawi, T. J., Rajiv, P., Mengelzadeh, N., Mohammed, I. A., & Balarak, D. (2021). Development of sonophotocatalytic process for degradation of acid orange 7 dye by using titanium dioxide nanoparticles/graphene oxide nanocomposite as a catalyst. *Journal of Environmental Management*, 292, Article 112777. <https://doi.org/10.1016/j.jenvman.2021.112777>
- American Public Health Association. (2017). *Standard methods for the examination of water and wastewater* (23rd ed.). American Public Health Association, American Water Works Association, and Water Environment Federation.
- Ayawei, N., Ebelegi, A. N., & Wankasi, D. (2015). Modelling and interpretation of adsorption isotherms. *Journal of Chemistry*, 2015, Article 412797.
- Babara, S., Gavade, N., Shinde, H., Gore, A. H., Mahajan, P., Lee, K. H., & Bhuse, V. (2019). An innovative transformation of waste toner powder into magnetic $g-C_3N_4-Fe_2O_3$ photocatalyst: Sustainable e-waste management. *Journal of Environmental Chemical Engineering*, 7, Article 103041. <https://doi.org/10.1016/j.jece.2019.103041>
- Balarak, D., Abasizadeh, H., Yang, J.-K., Shim, M. J., & Lee, S.-M. (2020a). Biosorption of Acid Orange 7 (AO7) dye by canola waste: Equilibrium, kinetic, and thermodynamic studies. *Desalination and Water Treatment*, 190, 331–339. <https://doi.org/10.5004/dwt.2020.25665>
- Balarak, D., Al-Musawi, T. J., Mohammed, I. A., & Abasizadeh, H. (2020b). The eradication of reactive black 5 dye liquid wastes using *Azolla filiculoides* aquatic fern as a good and economical biosorption agent. *SN Applied Sciences*, 2, Article 1015. <https://doi.org/10.1007/s42452-020-2841-x>
- Balarak, D., Ganji, F., Choi, S. S., Lee, S. M., & Shim, M. J. (2019). Effects of operational parameters on the removal of Acid Blue 25 dye from aqueous solutions by electrocoagulation. *Applied Chemistry and Engineering*, 30(6), 742–748. <https://doi.org/10.14478/ace.2019.1092>
- Balarak, D., Zafariyan, M., Igwegbe, C. A., Onyechi, K. K., & Ig-halo, J. O. (2021). Adsorption of Acid Blue 92 dye from aqueous solutions by single-walled carbon nanotubes: Isothermal, kinetic, and thermodynamic studies. *Environmental Processes*, 8(3), 869–888. <https://doi.org/10.1007/s40710-021-00505-3>
- Biver, C. (2021). Antimony in textile processing: Environmental concerns and sustainable approaches. *Journal of Hazardous Materials*, 415, Article 125589.
- Boparai, H. K., Joseph, M., & O'Carroll, D. M. (2011). Kinetics and thermodynamics of cadmium ion removal by adsorption onto

- nano zerovalent iron particles. *Journal of Hazardous Materials*, 186(1), 458–465. <https://doi.org/10.1016/j.jhazmat.2010.11.029>
- Bote, P. P., Vaze, S. R., Patil, C. S., Patil, S. A., Kolekar, G. B., Kurkuri, M. D., & Gore, A. H. (2021). Reutilization of carbon from exhausted water filter cartridges (EWFC) for decontamination of water: An innovative waste management approach. *Environmental Technology & Innovation*, 24, Article 102047. <https://doi.org/10.1016/j.eti.2021.102047>
- Chen, G., Lei, L., Hu, X., & Yue, P. L. (2003). Kinetic study on wet air oxidation of printing and dyeing wastewater. *Separation and Purification Technology*, 31, 71–76. [https://doi.org/10.1016/S1383-5866\(02\)00155-7](https://doi.org/10.1016/S1383-5866(02)00155-7)
- Cochrane, E. L., Lu, S., Gibb, S. W., & Villaescusa, I. (2006). A comparison of low-cost biosorbents and commercial sorbents for the removal of copper from aqueous media. *Journal of Hazardous Materials*, B137, 198–206. <https://doi.org/10.1016/j.jhazmat.2006.01.054>
- Crini, G. (2006). Non-conventional low-cost adsorbents for dye removal: A review. *Bioresource Technology*, 97(9), 1061–1085. <https://doi.org/10.1016/j.biortech.2005.05.001>
- Dąbrowski, A. (2001). Adsorption – from theory to practice. *Advances in Colloid and Interface Science*, 93(1–3), 135–224. [https://doi.org/10.1016/S0001-8686\(00\)00082-8](https://doi.org/10.1016/S0001-8686(00)00082-8)
- de Almeida, C. A., Silva, A. C., dos Santos, C. A., & de Souza, S. M. A. G. U. (2021). Optimization of Fenton and UV/H₂O₂ processes for the treatment of textile wastewater: Evaluation of toxicity and biodegradability. *Journal of Environmental Chemical Engineering*, 9(1), Article 104576.
- Devre, P. V., Patil, A. S., & Gore, A. H. (2023). Upcycling of spent granular carbon into a sustainable and recyclable biopolymeric hybrid hydrogel for highly efficient adsorptive removal of tetracycline pollutants from environmental waters and industrial effluents. *Journal of Environmental Chemical Engineering*, 11(2), Article 109368. <https://doi.org/10.1016/j.jece.2023.109368>
- Dhas, J. P. A. (2006). *Removal of color and COD from textile wastewater using limestone and activated carbon* [Master's thesis]. University of Science Malaysia, Malaysia.
- Dubinin, M. M., & Radushkevich, L. V. (1947). The equation of the characteristic curve of activated charcoal. *Proceedings of the Academy of Sciences USSR Physical Chemistry Section*, 55, 331–337.
- El Haddad, M., Mamouni, R., Saffaj, N., & Lazar, S. (2012). Removal of cationic dye – Basic Red 12 – from aqueous solutions by adsorption onto animal bone meal. *Journal of the Arab University Association for Basic and Applied Sciences*, 12(1), 48–54. <https://doi.org/10.1016/j.jaubas.2012.04.003>
- El Maguana, Y., Elhadiri, N., Bouchdoug, M., Benchanaa, M., & Jaouad, A. (2019). Activated carbon from prickly pear seed cake: Optimization of preparation conditions using experimental design and its application in dye removal. *International Journal of Chemical Engineering*, 2019, Article 8621951. <https://doi.org/10.1155/2019/8621951>
- Farhadi, A., Ameri, A., & Tamjidi, S. (2021). Application of agricultural waste as a low-cost adsorbent for removing heavy metals and dyes from wastewater: A review study. *Physical Chemistry Research*, 9(2), 211–226. <https://doi.org/10.22036/pcr.2021.256683.1852>
- Foo, K. Y., & Hameed, B. H. (2010). Insights into the modeling of adsorption isotherm systems. *Chemical Engineering Journal*, 156(1), 2–10. <https://doi.org/10.1016/j.cej.2009.09.013>
- Forgacs, E., Cserhati, T., & Oros, G. (2004). Removal of synthetic dyes from wastewaters: A review. *Environment International*, 30(7), 953–971. <https://doi.org/10.1016/j.envint.2004.02.001>
- Freundlich, H. (1906). Over the adsorption in solution. *The Journal of Physical Chemistry A*, 57(385471), 1100–1107.
- Gao, Y., Wang, Q. Y., Yue, J. C., & Wei, Q. (2007). Removal of color from simulated dye water and actual textile wastewater using composite coagulants made from poly ferric chloride and polydimethyldiallylammonium chloride. *Separation and Purification Technology*, 54, 157–163. <https://doi.org/10.1016/j.seppur.2006.08.026>
- Garba, Z. N., & Rahim, A. A. (2016). Efficient utilisation of durian seed biomass as an adsorbent for methylene blue: Isotherm, kinetics, and thermodynamic studies. *Journal of Environmental Chemical Engineering*, 4(4), 4461–4471.
- Georgiou, D., Hatiras, J., & Aivasidis, A. (2005). Microbial immobilization in a two-stage fixed-bed pilot plant reactor for on-site anaerobic decolorization of textile wastewater. *Enzyme and Microbial Technology*, 37, 597–605. <https://doi.org/10.1016/j.enzmictec.2005.03.019>
- Gunay, A., Arslankaya, E., & Tosun, I. (2007). Lead removal from aqueous solution by natural and pretreated clinoptilolite: Adsorption equilibrium and kinetics. *Journal of Hazardous Materials*, 146(1–2), 362–371. <https://doi.org/10.1016/j.jhazmat.2006.12.038>
- Gupta, K., Singh, R., & Pandey, P. (2011). Adsorption behavior of methylene blue on nano-cupric oxide: Effect of temperature and pH. *Journal of Hazardous Materials*, 186(1), 891–901.
- Gupta, N., Kushwaha, A. K., & Chattopadhyaya, M. C. (2012). Adsorptive removal of Pb²⁺, Co²⁺, and Ni²⁺ by hydroxyapatite/chitosan composite from aqueous solution. *Journal of Environmental Chemical Engineering*, 43, 125–131.
- Gupta, V. K., Suhas, A. I. M., & Saini, V. K. (2009). Removal of Rhodamine B, fast green, and methylene blue from wastewater using red mud, an aluminum industry waste. *Industrial & Engineering Chemistry Research*, 48(5), 2501–2509.
- Ho, Y. S. (2014). Comments on “Modeling the adsorption of chromium(VI) on guava leaves using response surface methodology” by Sharma and Kaur. *Environmental Science and Pollution Research*, 21(13), 8251–8253.
- Hui, Q., Lu, L.V., Pan, B.-C., Zhang, Q. J., Zhang, W.-M., & Zhang, Q.-X. (2009). Critical review of adsorption kinetic models. *Journal of Zhejiang University Science A*, 10, 716–724. <https://doi.org/10.1631/jzus.A0820524>
- Jiang, L., Zhang, W.-Z., Xu, Z.-F., Huang, H.-F., Ye, X.-X., Leng, B., Yan, L., Li, Z.-J., & Zhou, X.-T. (2016). M₂C and M₆C carbide precipitation in Ni-Mo-Cr based superalloys containing silicon. *Materials & Design*, 112, 300–308. <https://doi.org/10.1016/j.matdes.2016.09.075>
- Kadirvelu, K., Kavipriya, M., Karthika, C., Radhika, M., Vennilamani, N., & Pattabhi, S. (2003). Utilization of various agricultural wastes for activated carbon preparation and application for the removal of dyes and metal ions from aqueous solutions. *Bioresource Technology*, 87(1), 129–132. [https://doi.org/10.1016/S0960-8524\(02\)00201-8](https://doi.org/10.1016/S0960-8524(02)00201-8)
- Kalavathy, H. K., Regupathi, I., Pillai, M. G., & Miranda, L. R. (2009). Analysis and optimization of process parameters for activated carbon production from rubber wood sawdust using H₃PO₄. *Colloids and Surfaces B: Biointerfaces*, 70(1), 35–45. <https://doi.org/10.1016/j.colsurfb.2008.12.007>
- Karim, M. A., Nasir, S., Widowati, T. W., & Hasanudin, U. (2023). Kinetic study of adsorption of metal ions (iron and manganese) in groundwater using calcium carbide waste. *Journal of Ecological Engineering*, 24(5), 155–165. <https://doi.org/10.12911/22998993/161671>
- Khatibi, A. D., Yilmaz, M., Mahvi, A. H., & Balarak, D. (2022). Evaluation of surfactant-modified bentonite for Acid Red 88 dye

- adsorption in batch mode: Kinetic, equilibrium, and thermodynamic studies. *Desalination and Water Treatment*, 271, 48–57. <https://doi.org/10.5004/dwt.2022.28812>
- Kilic, M., Apaydin-Varol, E., & Pütün, A. E. (2011). Adsorptive removal of phenol from aqueous solutions on activated carbon prepared from tobacco residues: Equilibrium, kinetics, and thermodynamics. *Journal of Hazardous Materials*, 189(1–2), 397–403. <https://doi.org/10.1016/j.jhazmat.2011.02.051>
- Kose, T. E., & Kivanc, M. (2011). Adsorption of heavy metals from aqueous solutions using a novel agricultural waste material: Eggshell. *Journal of Environmental Sciences*, 23(9), 1548–1554.
- Kumar, K. V., Porkodi, K., & Rocha, F. (2010a). Isotherm and kinetic studies of methylene blue adsorption onto activated carbon prepared from wood waste. *Desalination*, 265(1–3), 147–156.
- Kumar, P. S., Ramalingam, S., Senthamarai, C., Niranjana, M., Vijayalakshmi, P., & Sivanesan, S. (2010b). Adsorption of dye from aqueous solution by cashew nut shell: Studies on equilibrium isotherm, kinetics and thermodynamics of interactions. *Desalination*, 261(1–2), 52–60. <https://doi.org/10.1016/j.desal.2010.05.032>
- Lambert, S. J., & Davy, A. J. (2011). Water quality as a threat to aquatic plants: Discriminating the effects of nitrate, phosphate, boron, and heavy metals on charophytes. *New Phytologist*, 189(4), 1051–1059. <https://doi.org/10.1111/j.1469-8137.2010.03543.x>
- Langmuir, I. (1918). The adsorption of gases on plane surfaces of glass, mica, and platinum. *Journal of the American Chemical Society*, 40(9), 1361–1403. <https://doi.org/10.1021/ja02242a004>
- Liakos, T. I., Sotiropoulos, S., & Lazaridis, N. K. (2017). Electrochemical and bioelectrochemical treatment of yeast wastewater. *Journal of Environmental Chemical Engineering*, 5, 699–708. <https://doi.org/10.1016/j.jece.2016.12.048>
- Maldonado, M., Malato, S., & Perez-Estrada, L. (2006). Partial degradation of five pesticides and industrial pollutants by ozonation in a pilot-plant scale reactor. *Journal of Hazardous Materials*, 138(2), 363–369. <https://doi.org/10.1016/j.jhazmat.2006.05.058>
- McKay, G., Blair, H. S., & Gardner, J. R. (1980). Adsorption of dyes on chitin. I. Equilibrium studies. *Journal of Applied Polymer Science*, 25(3), 581–591.
- Miler, M., Kočí, V., & Dvořák, L. (2016). Modeling of adsorption processes in water treatment: Equilibrium, kinetics and mass transfer. *Chemical Engineering Transactions*, 47, 397–402.
- Momina, B., Khan, S. J., & Shabana. (2020). Regeneration performance of bentonite clay in adsorption of dyes: Evaluation over multiple cycles. *Environmental Technology & Innovation*, 18, Article 100774.
- Mostafapour, F. K., Yilmaz, M., Mahvi, A. H., Younesi, A., Ganji, F., & Balarak, D. (2022). Adsorptive removal of tetracycline from aqueous solution by surfactant-modified zeolite: Equilibrium, kinetics, and thermodynamics. *Desalination and Water Treatment*, 247, 216–228. <https://doi.org/10.5004/dwt.2022.27943>
- Patil, C. S., Gunjal, D. B., Naik, V. M., Harale, N. S., Jagadale, S. D., & Gore, A. H. (2019). Waste tea residue as a low-cost adsorbent for removal of hydralazine hydrochloride pharmaceutical pollutant from aqueous media: An environmental remediation. *Journal of Cleaner Production*, 206, 407–418. <https://doi.org/10.1016/j.jclepro.2018.09.140>
- Patil, C. S., Kadam, A. N., Gunjal, D. B., Naik, V. M., Lee, S.-W., Kolekar, G. B., & Gore, A. H. (2020). Sugarcane molasses derived carbon sheet@sea sand composite for direct removal of methylene blue from textile wastewater: Industrial wastewater remediation through sustainable, greener, and scalable methodology. *Separation and Purification Technology*, 247, Article 116997. <https://doi.org/10.1016/j.seppur.2020.116997>
- Pirkarami, A., & Olya, M. E. (2017). Removal of dye from industrial wastewater with an emphasis on improving economic efficiency and degradation mechanism. *Journal of Saudi Chemical Society*, 21, S179–S186. <https://doi.org/10.1016/j.jscs.2013.12.008>
- Raji, M., Mirbagheri, S. A., Ye, F., & Dutta, J. (2021). Nano zero-valent iron on activated carbon cloth support as Fenton-like catalyst for efficient color and COD removal from melanoidin wastewater. *Chemosphere*, 263, Article 127945. <https://doi.org/10.1016/j.chemosphere.2020.127945>
- Rauf, M. A., & Ashraf, S. S. (2012). Survey of recent trends in biochemically assisted degradation of dyes. *Journal of Chemical Engineering*, 209, 520–530. <https://doi.org/10.1016/j.ccej.2012.08.015>
- Senthilkumaar, S., Varadarajan, P. R., Porkodi, K., & Subbhuraam, C. V. (2006). Adsorption of methylene blue onto jute fiber carbon: Kinetics and equilibrium studies. *Journal of Colloid and Interface Science*, 284(1), 78–82. <https://doi.org/10.1016/j.jcis.2004.09.027>
- Shinde, S. B., Dhengale, S. D., Nille, O. S., Jadhav, S. S., Gore, A. H., Bhosale, T. R., Birajdar, N. B., Kolekar, S. S., Kolekar, G. B., & Anbhule, P. V. (2023). Template-free synthesis of mesoporous carbon from firecracker waste and designing of ZnO-Mesoporous carbon photocatalyst for dye (MO) degradation. *Inorganic Chemistry Communications*, 147, Article 110242. <https://doi.org/10.1016/j.inoche.2022.110242>
- Taty-Costodes, V. C., Fauduet, H., Porte, C., & Delacroix, A. (2003). Removal of Cd(II) and Pb(II) ions, from aqueous solutions, by adsorption onto sawdust of *Pinus sylvestris*. *Journal of Hazardous Materials*, 105(1–3), 121–142. <https://doi.org/10.1016/j.jhazmat.2003.07.009>
- Toth, J. (2002). *Adsorption: Theory, modeling, and analysis*. Marcel Dekker, Inc.
- Vimala, R., & Das, N. (2009). Biosorption of cadmium (II) and lead (II) from aqueous solutions using fungi: A comparative study. *Journal of Hazardous Materials*, 168(1), 376–382. <https://doi.org/10.1016/j.jhazmat.2009.02.062>
- Vunain, E., Mishra, A. K., & Krause, R. W. (2013). Fabrication, characterization, and application of polymer nanocomposites for arsenic(III) removal from water. *Journal of Inorganic and Organometallic Polymers and Materials*, 23(2), 293–305. <https://doi.org/10.1007/s10904-012-9775-8>
- Weber, W. J., & Morris, J. C. (1963). Kinetics of adsorption on carbon from solution. *Journal of the Sanitary Engineering Division*, 89(2), 31–59. <https://doi.org/10.1061/JSEDAI.0000430>
- Yagub, M. T., Sen, T. K., Afroze, S., & Ang, H. M. (2014). Dye and its removal from aqueous solution by adsorption: A review. *Advances in Colloid and Interface Science*, 209, 172–184. <https://doi.org/10.1016/j.cis.2014.04.002>
- Zhang, X., Wang, Y., Wang, J., Zhang, Y., & Zhang, D. (2019). Temperature effects on adsorption of pollutants from wastewater: A review. *Chemical Engineering Journal*, 374, 1454–1464.
- Zhou, Y., Lu, J., Zhou, Y., & Liu, Y. (2019). Recent advances for dyes removal using novel adsorbents: A review. *Environmental Pollution*, 252, 352–365. <https://doi.org/10.1016/j.envpol.2019.05.072>